


RESEARCH ARTICLE

A familial Alzheimer's disease associated mutation in presenilin-1 mediates amyloid-beta independent cell specific neurodegeneration

Mahraz Parvand¹ , Joseph J. H. Liang¹ , Tahereh Bozorgmehr¹, Dawson Born¹, Alvaro Luna Cortes¹, Catharine H. Rankin^{1,2*} 

1 Djavad Mowafaghian Centre for Brain Health, University of British Columbia, Vancouver, British Columbia, Canada, **2** Department of Psychology, University of British Columbia, Vancouver, BC, Canada

 These authors contributed equally to this work.

* crankin@psych.ubc.ca



OPEN ACCESS

Citation: Parvand M, Liang JJH, Bozorgmehr T, Born D, Luna Cortes A, Rankin CH (2024) A familial Alzheimer's disease associated mutation in presenilin-1 mediates amyloid-beta independent cell specific neurodegeneration. PLoS ONE 19(9): e0289435. <https://doi.org/10.1371/journal.pone.0289435>

Editor: Efthimios M. C. Skoulakis, BSRC Alexander Fleming: Biomedical Sciences Research Center Alexander Fleming, GREECE

Received: July 17, 2023

Accepted: August 23, 2024

Published: September 6, 2024

Copyright: © 2024 Parvand et al. This is an open access article distributed under the terms of the [Creative Commons Attribution License](https://creativecommons.org/licenses/by/4.0/), which permits unrestricted use, distribution, and reproduction in any medium, provided the original author and source are credited.

Data Availability Statement: The data underlying the results presented in the study are available on OSF project repository (URL: https://osf.io/fzq8c/?view_only=6ad235a75d1443a692f6504e75a48667).

Funding: This research was supported by a Canadian Institutes of Health Research Institute of Neurosciences, Mental Health and Addiction Grant #PJT 165947 to CHR, MP was supported by the

Abstract

Mutations in the presenilin (*PS*) genes are a predominant cause of familial Alzheimer's disease (fAD). An ortholog of *PS* in the genetic model organism *Caenorhabditis elegans* (*C. elegans*) is *sel-12*. Mutations in the presenilin genes are commonly thought to lead to fAD by upregulating the expression of amyloid beta ($A\beta$), however this hypothesis has been challenged by recent evidence. As *C. elegans* lack amyloid beta ($A\beta$), the goal of this work was to examine $A\beta$ -independent effects of mutations in *sel-12* and *PS1/PS2* on behaviour and sensory neuron morphology across the lifespan in a *C. elegans* model. Olfactory chemotaxis experiments were conducted on *sel-12(ok2078)* loss-of-function mutant worms. Adult *sel-12* mutant worms showed significantly lower levels of chemotaxis to odorants compared to wild-type worms throughout their lifespan, and this deficit increased with age. The chemotaxis phenotype in *sel-12* mutant worms is rescued by transgenic over-expression of human wild-type *PS1*, but not the classic fAD-associated variant *PS1_{C410Y}*, when expression was driven by either the endogenous *sel-12* promoter (*Psel-12*), a pan-neuronal promoter (*Primb-1*), or by a promoter whose primary expression was in the sensory neurons responsible for the chemotaxis behavior (*Psra-6*, *Podr-10*). The behavioural phenotype was also rescued by over-expressing an atypical fAD-linked mutation in *PS1* (*PS1_{ΔS169}*) that has been reported to leave the Notch pathway intact. An examination of the morphology of polymodal nociceptive (ASH) neurons responsible for the chemotaxis behavior also showed increased neurodegeneration over time in *sel-12* mutant worms that could be rescued by the same transgenes that rescued the behaviour, demonstrating a parallel with the observed behavioural deficits. Thus, we report an $A\beta$ -independent neurodegeneration in *C. elegans* that was rescued by cell specific over-expression of wild-type human presenilin.

Ecole Polytechnique Commemorative Award from the Canadian Federation of University Women (CFUW), JL was supported by an NSERC PGS-D. The funders had no role in study design, data collection and analysis, decision to publish, or preparation of the manuscript.

Competing interests: The authors have declared that no competing interests exist.

Introduction

There are a variety of disorders that lead to impaired memory and cognition among older adults, of which Alzheimer's disease (AD) is the most common, accounting for 60% of all dementias [1]. The majority of AD and related dementias are chronic illnesses; they appear in stages, and patients' symptoms worsen with time [2]. There are two forms of AD: sporadic AD where genetic risk factors are inherited in a non-Mendelian fashion, and familial AD (fAD) where genetic risk factors are autosomal dominant [3]. Familial AD presents earlier than the sixth or seventh life decade and is much less prevalent than AD, however, because fAD offers known genetic causes, this form of the disorder has been the target of much research. Mutations in three genes have been linked to a majority of fAD cases: presenilin 1 (*PS1*), and presenilin 2 (*PS2*) and amyloid precursor protein (*APP*; [4]). Although these genes each alter a large number of cellular processes, multiple studies have focussed on a two common effects: mutations in any one of these genes lead to increased production of amyloid-beta ($A\beta$) and inflammation [5].

The presenilins have a number of intracellular functions; the most commonly studied is their role as the catalytic subunit of γ -secretase, a protein responsible for the proteolysis of many proteins including APP and Notch [6]. To date, more than 350 PS1 mutations have been reported in AD patients [7]. A second protein, PS2, has significant homology to PS1 at both gene and protein levels and has also been identified as a cause of fAD [8]. Mutations in PS2 account for the smallest percentage of fAD cases and lead to a later age of onset compared to PS1 and APP mutations [4]. In the clinic, the majority of presenilin mutations identified in patients are missense substitutions that present an autosomal dominant inheritance pattern. As dominant phenotypes typically imply a gain-of-function mechanism, it is believed that pathogenic mutations in PS lead to a toxic gain-of-function phenotype that increases $A\beta_{42}/A\beta_{40}$ ratios, a well-known biomarker of AD [9]. However, more recent analysis using mammalian cells has shown that while a vast majority of the studied PS1 mutations do lead to increased $A\beta_{42}/A\beta_{40}$ ratios, a majority of these variants significantly decrease production of both $A\beta_{42}$ and $A\beta_{40}$ and have no significant correlation to mean age at onset of fAD for the corresponding mutations [10], casting doubt on the widely accepted assumption that pathogenic PS1 variants lead to fAD by favoring production of $A\beta_{42}$ over $A\beta_{40}$.

In studies of the underlying causes of AD, APP has been a major focus of research. The amyloid hypothesis was formalized for the first time in 1992 when Hardy and Higgins proposed that the build-up of plaques containing $A\beta$ is the predominant cause of AD [11]. Since then, many studies have attempted to determine how amyloid plaques lead to AD and whether elimination of plaques would cure AD. Thus far, research on amyloid plaques has not led to clear answers or to an effective treatment for AD. Although amyloid plaques are considered a hallmark of AD, a build-up of amyloid peptides can also be part of normal aging as $A\beta$ plaques are apparent in 45% of cognitively normal elderly individuals [12]. Because the strongest predictor of both $A\beta$ build up and AD is aging, it may be that other aging-related issues combine with the build-up of amyloid plaques to trigger AD. Since the aggregation of $A\beta$ plaques cannot, on its own, be the sole causal mechanism underlying AD, researchers are exploring the notion that AD is a complex disorder and that multiple pathways other than amyloid plaques may produce the disease characteristics [13].

Because of the known role of presenilins in processing APP, much of the research done on *PS1/PS2* is within the context of processing APP. Mouse models containing only *PS1* or *PS2* mutations show an increased proportion of $A\beta_{42}$ but do not exhibit amyloid plaques, thus numerous rodent studies investigating PS1 have used double transgenic mice that have mutations in both *APP* and *PS1* transgenes [14,15]. Plaque formation and cognitive impairment

phenotypes manifest much earlier and much more extensively in these double transgenic lines, compared to *APP* transgenic lines without *PS1/PS2* mutations or transgenes [14].

Somewhat less studied in rodents are phenotypes in transgenic lines expressing only presenilin mutations, possibly due to lack of complete AD-like pathology. However, recent rodent work has shown that *PS1* and *PS2* fAD transgenic lines show a plethora of phenotypes, including increased susceptibility to hippocampal damage from kainite induced excitotoxicity or trimethyltin treatment, increased protein oxidation and lipid peroxidation in the mutant brain, impaired hippocampal neurogenesis in adult mice and an age-dependent impairment of spine morphology and synaptic plasticity in hippocampal neurons [15,16]. Partial or complete loss of presenilin by the knock-out of both *PS1* and *PS2* leads to age-dependent neurodegeneration in the mouse brain [17–19], and in another *PS1* knock-in line aging-dependent neurodegeneration and neuronal loss has also been observed [20]. In electrophysiological studies, *PS1* fAD mutations were found to alter long-term potentiation (LTP) in the hippocampus [16]. In studies comparing very young transgenic mice over-expressing an fAD mutation in *PS1* to counterparts over-expressing wild-type *PS1*, fAD mutants showed enhanced LTP. However, at 8–10 months of age LTP was similar to wild-type mice, and at 13–14 months of age LTP was significantly decreased [16]. Pharmacological blocking studies also showed that the fAD-associated *PS1* mutants altered NMDA receptor-mediated neurotransmission [21]. Behavioural experiments in young mice have also shown that *PS1* fAD transgenic mice have behavioural impairments, although the deficits observed are somewhat subtle and inconsistent [16]. Taken together, there is evidence to suggest an alternate hypothesis that loss-of-function mutations in the presenilin genes can elicit AD pathology through one or more molecular pathway(s) independent from that for processing APP [22].

Another proteolytic target for γ -secretase is Notch. Alterations in Notch proteolysis by mutations in *PS1* that affect γ -secretase may also be involved in AD pathogenesis. The Notch protein is a type I transmembrane cell surface receptor that plays a role in cell fate decisions of both vertebrates and invertebrates [23,24]. Binding to a member of the Delta, Serrate, or Lag2 (DSL) family of ligands triggers Notch proteolysis, leading to the cleavage of Notch by many of the same secretases that cleave APP [25]. Notch is expressed in neurons at especially high levels in the hippocampus in the adult rodent brain [26], and in some rodent models with presenilin deficiencies, Notch loss-of-function phenotypes are observed [27,28]. Thus, there is evidence to suggest that alterations in Notch can be a contributing factor to AD pathogenesis in the context of *PS1*. To date the role of Notch signaling in AD pathogenesis remains largely unclear.

In the present study, we used the roundworm *Caenorhabditis elegans* (*C. elegans*) to investigate the role of *PS1* and Notch in neural degeneration and relevant behavioral impairments produced by a mutation in *sel-12*, an orthologue of *PS1*. *SEL-12* shares approximately 50% amino acid identity with human *PS1*, among which include many AD-associated residues. As *C. elegans* express two genes orthologous to human Notch receptors, *glp-1* and *lin-12*, questions regarding Notch signaling in the context of fAD can be interrogated in this model system as well. There are a number of advantages to using *C. elegans* for studying neurological degenerative diseases including its short life span (14–18 days), a sequenced genome, and defined nervous system with 302 identified neurons that are well characterized with a mapped connectome [29]. Basic cellular neurobiological functions are well conserved, with *C. elegans* having cellular and biochemical processes similar to those in mammals. The first known function of presenilins was the role of *PS1* in cleaving Notch based on the observation that mutations in *sel-12* produced an egg-laying deficit known to be caused by impaired Notch signaling [30]. *C. elegans* shows both genetic and functional similarity with orthologs of many of the mammalian neurotransmitters (e.g., dopamine, serotonin, GABA, glutamate, acetylcholine, and their receptor subtypes) and many classes of ion channels (e.g., sodium, calcium, and potassium

channels) [31]. In fact, in addition to PS1, a number of human genes associated with AD have *C. elegans* orthologs [32]. However, it is important to acknowledge that the *C. elegans* ortholog of APP, *apl-1*, does not generate a product orthologous to A β nor does the nematode system have an ortholog of BACE-1 encoding β -secretase [29]. Whereas the human APP protein may undergo two primary proteolytic pathways (the non-amyloidogenic involving the α - and γ -secretases, and the amyloidogenic pathway involving β - and γ -secretases), the orthologous nematode system has only the orthologous proteolytic components for the non-amyloidogenic pathway. However, besides lacking a β -secretase and an orthologous A β sequence, the APP processing pathway is largely conserved [33,34] with experimental evidence suggesting that SEL-12 regulates the activity of APL-1 [35]. Therefore, the nematode model offers a unique opportunity for studying functions of presenilins in an A β -free biological system.

Here we studied whether mutations in *sel-12* altered chemotaxis and sensory neuron morphology across aging, and whether deficits could be rescued by over-expressing variants of human PS1. To do this we first tested olfactory chemotaxis across development and during aging in *sel-12* mutant worms, and in worms over-expressing either human wild-type PS1 or one of the two PS1 mutations: PS1_{C410Y}, a classical fAD mutation that impairs both A β and Notch processing, [36,37], and a novel mutation, PS1 Δ _{S169}, which is believed to impair A β but leave Notch processing intact [38]. In *sel-12* mutants and worms over-expressing the PS1 transgenes, we also assessed whether there was neurodegeneration of the ASH chemosensory neurons that are responsible for sensing the odorant used in our chemotaxis assay. We found that in *sel-12* mutant worms, there was more degeneration of the ASH sensory neurons with increasing age and this degeneration could be rescued by both nervous system and cell-specific expression of wild-type PS1 and PS1 Δ _{S169}, but not PS1_{C410Y}. These results show an A β -independent, cell specific role of presenilin in neuronal degeneration.

Materials and methods

Generation of transgenic lines and strain maintenance

C. elegans Bristol wild-type (N2), *sel-12(ok2078)* mutant (RB1672), and the transgenic nuIs [*osm-10::GFP+lin-15(+)*] (HA3) strains were provided by the Caenorhabditis Genetics Center (CGC), and the transgenic strain HA1712 (*lin-12 (null)*; *Phsp-16.2::gfp-1RNAi*) was provided graciously by Dr. Anne Hart of Brown University. Worms were cultured on *Escherichia coli* (*E. coli*) seeded nematode growth medium (NGM). All experiments were conducted in 6cm Petri plates that were filled with 10 mL NGM agar a maximum of two weeks prior to use. Worms were stored in a 20°C incubator and all experiments were conducted in a room with controlled humidity (40±5% RH) and temperature (20±1°C).

Transgenic overexpression lines were constructed by microinjection of DNA plasmids into the germ line of young adult *sel-12* mutant worms at a concentration of 10 ng/ μ l along with a co-injection GFP marker [39]. This DNA mixture was injected into the distal arm of the worm's gonad, which contains a central cytoplasm core that is shared by germ cell nuclei [39]. Worms were injected under an inverted Zeiss DIC microscope equipped with a 40X Nomarski objective. The plasmid pBY140 containing the wild-type PS1 coding region expressed by the *sel-12* promoter was provided by Dr. Ralf Baumeister (Albert-Ludwig University in Freiburg/Breisgau, Germany). To generate pan-neuronal, ASH-specific and AW-specific over-expression constructs, promoter regions of *rimb-1* (2.6kb fragment, 734bp upstream of start codon, from pSF11[*ptag-168p::nCre*]), *sra-6* (1.8kb fragment, 158bp upstream of start codon) and *odr-10* (986bp fragment, 28bp upstream of start codon), respectively were used to replace the *sel-12* promoter region in the original pBY140 via restriction cloning. Lines with >50% GFP transmission were selected for testing. Because DNA microinjection creates an extra-

chromosomal array, there is inherent variability of expression levels because there were probably different copy numbers of plasmids incorporated into the array and there was also the possibility of different cells having different genotypes (mosaic expression) [40]. To overcome this, three independent lines for each construct were tested [41]. Please refer to [S1 Table](#) for a full list of strains generated and tested.

Chemotaxis assays

To ensure that all animals tested were the same developmental age, adult worms ($n = 20\text{--}30$) were placed in a droplet of 4 μ l of bleach solution (1:1 ratio of 100% bleach and 1M NaCl). The worms' bodies disintegrated but their eggs survived. All eggs hatched at roughly the same time, and larvae were allowed to grow for three days on agar seeded with *E. coli* in a 20°C incubator. On day three, 72-hour post egg-lay worms were collected using 700 μ l of liquid M9 buffer into 1.5mL centrifuge tubes. To remove OP50 *E. coli* from the bodies of the worms, worms were centrifuged for a minute at 1000rcf and the supernatant was removed. Another 700 μ l of M9 buffer was added to the tubes, and the worms were centrifuged again (done 3 times). After the third time, the supernatant was removed and the pellet of the worms remained in the tube.

The chemotaxis procedure used was adapted from Margie *et al.* [42]. Eight NGM Petri plates (6cm diameter) were used per strain (4 control, 4 test) and each was divided into four equal quadrants. In the center of each plate a circle of 1cm diameter ([Fig 1A](#)) was drawn on the bottom of the plate and lines were drawn to mark the quadrants. For test plates, each quadrant was marked as control or test. For control plates, all 4 quadrants were labelled as control. The octanol solution was prepared by mixing of a 1:1 ratio of 100% octanol and 1M-sodium azide (NaN_3) that was used to immobilize worms. The diacetyl solution was prepared by diluting it to 0.5% diacetyl using 99.5 μ l of M9 and 5 μ l of diacetyl. A 1:1 ratio of this 0.5% diacetyl solution was then added to NaN_3 . Control solution was prepared by mixing equal volumes of M9 and NaN_3 . Washed worms (50–100) were pipetted into the circle at the center of the plates. Then 2 μ l of the volatile odorants octanol or diacetyl were placed on spots located at the centre of the test quadrants, and 2 μ l of the control solution was placed on spots located at the centre of the control quadrants ([Fig 1A](#)).

Plate lids were kept open for approximately 15 minutes until the odorants soaked into the agar and the surface of the agar appeared dry. Worms were then left to move around the plates undisturbed for one hour in a 20°C room. Plates were then transferred into a 4°C refrigerator for two hours to immobilize worms before counting. Prior to counting plates were relabeled and a key generated, plates were removed from the refrigerator for counting one at a time and the number of worms in each quadrant was counted by a researcher blind to the condition/strain/the study objectives. After counting the blind was broken and a chemotaxis index (CI) was calculated ([Fig 1A](#)).

Use of 5'-fluorodeoxyuridine (FUdR) in aging studies

Because *sel-12* mutant worms have an egg-laying deficit, eggs accumulate inside the gonad and the progeny hatch inside the adult killing it at a relatively young age (Leviton *et al.*, 1995). This makes studies using older worms difficult. To stop the hatching of eggs inside adults so the adults lived to an older age, we used 5'-fluorodeoxyuridine (FUdR). FUdR is an inhibitor of DNA synthesis that is used in *C. elegans* lifespan studies to preserve a synchronized aging population [43]. Two days prior to adding *E. coli* to NGM plates, 250 μ l of 100 μ M FUdR was spread on plates. Two days after the addition of *E. coli*, Larval stage 4 (L4, approx. 50 hours post hatch) animals were transferred to the NGM plates with FUdR. For aging studies, adult worms

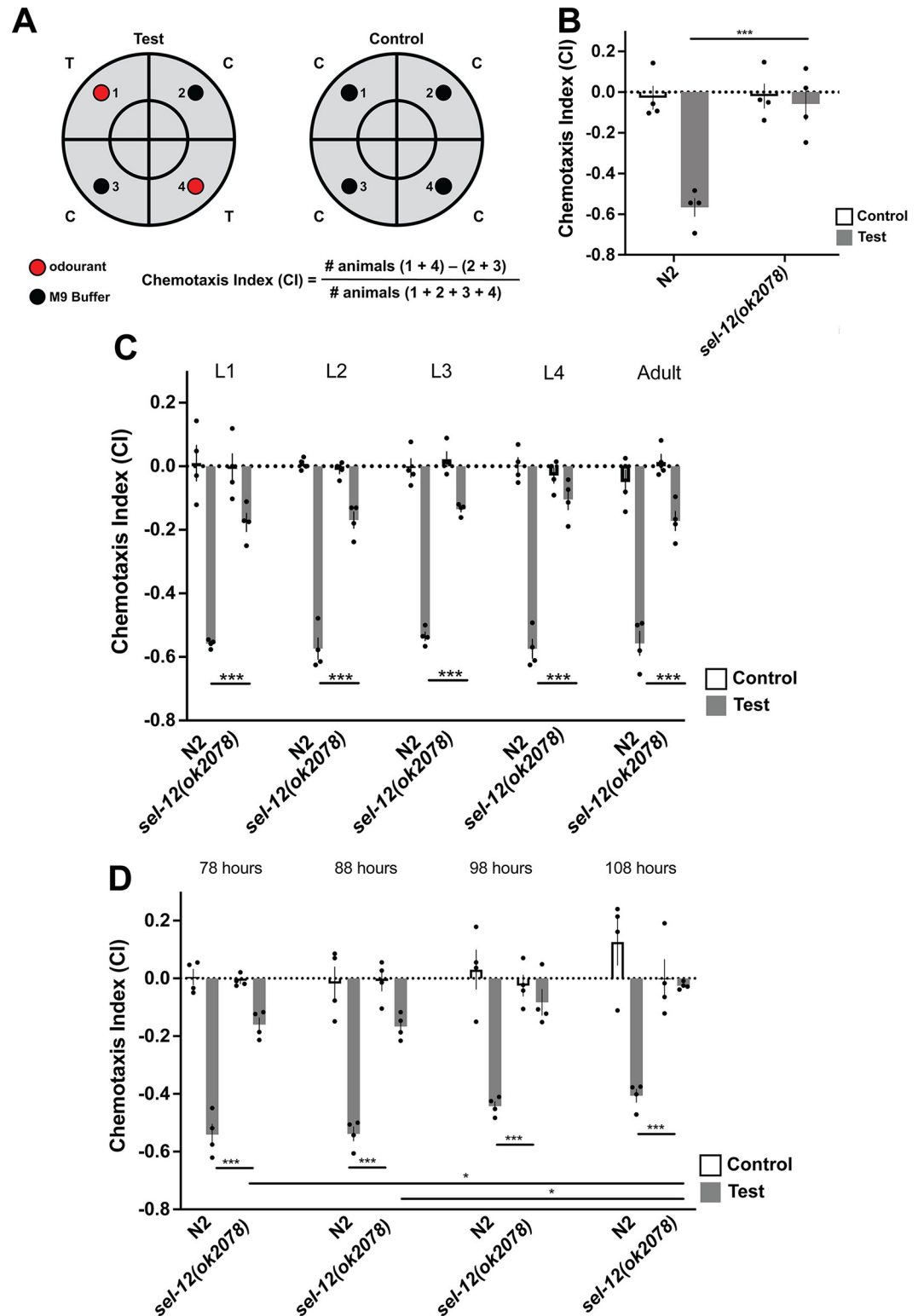


Fig 1. Worms with mutations in orthologs of *PS1* show progressive chemosensory impairments. A) Chemotaxis assay—worms are placed in the centre circle and allowed 1 hour to navigate plate. Anesthetic is included in buffer and odorant spots, so worms remain at the quadrant of choice. Worms in each quadrant are counted and CI calculated as shown. B) at 72 hours post egg-lay, young adult *sel-12* mutants display impaired octanol avoidance behavior. C) *sel-12* chemotaxis deficits are present from hatch. D) *sel-12* chemotaxis deficits become more severe with age. At 78 hours post egg-lay worms are egg

laying adults. They continue to lay eggs for 3–4 days. By 7 days post egg-lay worms are progressing into old age. Each bar represents an average from 4 independent plates ($n = 50$ – 100 worms per plate). Independent plate CI are shown as circles. White bars represent control plates and black bars represent test plates. Error bars reflect the standard error of the mean. *** $p < 0.001$, * $p < 0.05$.

<https://doi.org/10.1371/journal.pone.0289435.g001>

were tested at 10 hour intervals from 78 to 108 hours post egg-lay (young adult to senior worms). In experiments where FUdR was used all genotypes were treated with FUdR, including the wild-type control.

Locomotion assay

Behavioral experiments on worms of different ages were used to determine speed and the locomotory ability of worms on plates to ensure they were able to chemotax to the test spots in the time given. The multi-worm tracker (MWT) is an automated machine vision system that records features of worm behavior for many worms simultaneously; for this assay crawling speed was measured [44]. To assess locomotion, approximately 50 worms of each age were hand-picked onto a plate without FUdR or *E. coli* ($n = 3$ plates), placed on the MWT, and the lid of each plate was lifted briefly to provide an air-puff stimulus to arouse worms so they were moving and could be recognized by the MWT. Worms were tracked for 250 seconds.

Knock-down of both Notch receptors via heat shock and developmental stage synchronization

Because worms carrying null mutations in both *glp-1* and *lin-12* have a lethal phenotype, we studied the effect of double loss-of-function of both Notch receptors by the adulthood induction of *glp-1* RNAi knockdown using a heat-shock promoter (*hsp-16.2*) in a *lin-12(n941)* null mutant background. Animals with a heat shock promoter driving *glp-1* RNAi were raised at 15°C, the permissive temperature. During heat-shock experiments, all strains used, including wild-type, were moved to 33°C, the restrictive temperature, for 2 hours as described in Singh *et al.* [45] After this, animals were allowed to recover for 3 hours in a 20°C incubator prior to chemotaxis experiments that were conducted in a 20°C behavior room. Expression levels of *hsp-16.2* persist even up to 50 hours after heat shock [46], suggesting that after 3 hours of recovery there would still be sufficient knockdown of *glp-1*. Note that Notch mutant worms have developmental delays compared to wild-type. To test worms at similar stages in development, wild-type and *lin-12/glp-1* deficient worms were closely observed every 4 hours to determine when these strains reached young adulthood (defined as containing at least 4 eggs [47]). Compared to wild-type worms, worms with deficiencies in both Notch receptors had a 6-hour lag in development (reached young adults at 68 hours in 20°C).

ASH neuron imaging

The single pair of ASH sensory neurons in the head of the worm are the primary chemosensory receptors for detecting octanol. For imaging we used strains expressing *Posm-10::GFP* that filled the ASH neuron cell bodies and processes with GFP and imaged both wild-type and *sel-12* mutant worms over time (78, 98, and 108 hour old worms). For all extrachromosomal rescue strains, the line that had the closest chemotaxis index to wild-type was chosen for imaging. The researcher doing the imaging was blind to the strains being imaged. Worms were placed on 2% agar pads on sterile glass microscope slides in 15 μ L of 50mM NaN₃ for immobilization. Worms were given approximately one minute to become immobile prior to being covered with a 1.5mm thick coverslip. Images were obtained using a Leica SP8 white light

confocal microscope. To excite GFP, a 488nm wavelength laser was used and the emitted light was collected by passing through a 510-550nm bandpass filter. Depending on the thickness of the worm and the brightness of its GFP, optical sections were collected at various intervals using a 63X oil immersion lens and summed into a single Z projected image. Neurons were quantified using the Fiji: ImageJ Software.

Independent groups of one hundred worms were imaged per strain at 78, 98 and 108 hours of age for a total of 300 images per strain. During analysis, ASH neuron morphology was classified into three categories: normal, gapped/missing arm, and bleb. If gaps and blebs were both present, the neuron would be categorized as blebs.

For DiI dye-filling experiments, animals were collected and incubated in 400 μ L 1.25 μ M DiI in the dark for 30 minutes. After incubation, worms were transferred back onto OP-50 seeded NGM plates for 30 minutes then collected for imaging.

Statistical analysis

Data are reported as means \pm standard error of the mean (SEM) of three or four independent plates with 50–100 worms on each for each strain tested. Because expression levels from extrachromosomal transgenes can be variable, we analyzed data for 3 independent lines of each transgene. For the sake of clarity, we report analysis for our collapsed data. The presenilin rescue strains are reported as the average of four plates for each of three extrachromosomal lines (total of 12 plates). Each rescue line was analyzed independently and then as averages of the three extrachromosomal rescue lines for each strain. Data analyses were conducted using the GraphPad Prism software, SPSS and python (pingouin 0.5.1). Data were checked for normal distribution and one-tailed independent T tests were conducted for pair-wise comparisons. In experiments with three or more groups, a one-way ANOVA was conducted with a Tukey's Honest Significant Difference test with statistical significance set at $p = 0.05$ for post-hoc analyses. The percentage of normal and abnormal ASH morphology of each strain was compared to other strains using aggregated Pearson's chi-squared test. P values of less than 0.05 were considered significant. Data visualization was done with GraphPad Prism, Python (with Plotly 5.7.0 graphing library) and Adobe Illustrator.

Results

C. elegans with a *sel-12* mutation displayed olfactory impairments shortly after hatching that increased over time

In *C. elegans*, there are three members of the Presenilin family: *hop-1*, *sel-12*, and *spe-4* [41,48,49]. *spe-4* is only distantly related to human presenilins and is expressed only in the male germline [48], and thus was not investigated in this work. Although both *hop-1* and *sel-12* are homologous in terms of protein structure and domain similarity to human PS1, are widely expressed throughout the worms [30] and have been shown to function redundantly in facilitating the Notch pathway through *lin-12* and *glp-1* signalling [49–51], *hop-1* is considered more diverged from SEL-12 and PS1 (31% sequence homology to human PS1 compared to 50% for SEL-12). Additionally, of the 113 PS1 residues where pathogenic and likely pathogenic occur, only 45 (40%) are conserved in HOP-1 whereas 89 (79%) are conserved in SEL-12 (S1 Fig). Critically, whereas *sel-12* is strongly expressed in the neurons studied in our experiments (ASH and AWA), *hop-1* is not [52]. Thus, we focused our work on a strain of worms expressing a putatively null *sel-12(ok2078)* deletion allele.

To assess the olfactory abilities of wild-type and *sel-12* mutant worms across the lifespan we examined them across development. *C. elegans* have 4 larval stages (lasting from ~12–24 hrs in

length) and we tested the aversive chemotactic response to octanol at each stage, L1-L4, as well as at 72 hours post egg-lay (reproductive young adult worms; Fig 1B). Compared to wild-type worms, *sel-12* mutants had significant chemotaxis index deficits from L1 that were also seen in L2, L3, L4, and adult worms [$F(9, 30) = 65.60$, $p < 0.001$] (Fig 1C). This finding was surprising, as past observations noted that chemotaxis towards food was not effected in *sel-12* mutants [51].

We also tested whether the olfactory deficits progressed with advanced age by testing worms ranging in age from reproductive adult to old age at 10 hour intervals (78–108 hours post egg-lay; Fig 1D). The multivariate analysis of covariance showed a significant group effect indicating there was a significant difference in CI scores between groups ([$F(7, 24) = 60.11$, $p < 0.001$]). Post-hoc analyses showed that although there was a mild but non-significant pattern of decrease in chemotaxis index over time between 78 hours old and 108 hours old in wild-type worms ($p = 0.06$), the decrease in chemotaxis index was much more rapid and was significant in *sel-12* mutant worms across age (Fig 1D; $p = 0.05$). Overall, wild-type and *sel-12* mutant worms had chemotaxis index decrements from 78 to 108-hours old of 15% and 81%, respectively.

Motor ability is not a confounding variable in *sel-12(ok2078)* mutant chemotaxis

It is possible that the egg-laying phenotype of the *sel-12* mutants could lead to bloating and impair the ability to locomote well enough to successfully chemotax within the allotted time. We investigated this possibility by assessing locomotor speed of wild-type and *sel-12* worms at 68hr, 78hr, 88hr, 98hr and 108hrs of age on the MWT, in a neutral *E. coli* (OP-50) seeded environment without any odourants. Although at 68 hours old *sel-12* mutant worms appeared slower than wild-type by visual observation, via MWT analyses average forward speed during the entire tracking session was not significantly different (S2A Fig; $p = 0.08$). In comparing worms aged from 68 hours to 108 hours old, wild-type worms' forward speed peaked at 88 hours and slowed down at 108 hours old. In contrast, the speed of *sel-12* mutant worms did not increase from 68 hours to 88 hours old and was significantly slower at 88-hour ($t(4) = 5.89$, $p = 0.002$) and 98-hour old ($t(4) = 6.10$, $p = 0.002$) compared to wild-type worms (S2A Fig). Despite the observation that *sel-12* mutant worms move more slowly than wild-type worms, they were able to navigate around the entire petri plate within approximately 5 minutes (S2B Fig), demonstrating that they could exhibit chemotaxis behavior in the 1-hour test session if they were able to detect the olfactory cue. Thus, despite a marked reduction in locomotion speed in comparison to their wild-type counterparts, *sel-12* mutants maintained sufficient locomotor ability to explore and navigate to all areas of the plate environment in the given time.

Expression of wild-type *sel-12* and wild-type *PS1* rescued chemotaxis deficit when driven by the endogenous *sel-12* promoter

Using extrachromosomal arrays we over-expressed wild-type *sel-12* with its endogenous promoter (*Psel-12::sel-12*) in the *sel-12* mutant and showed that it rescued octanol chemotaxis behavior (Fig 2A; [$F(2,17) = 2.65$, $p < 0.001$]). Over-expressing human *PS1* driven by the *sel-12* promoter (*Psel-12::PS1_{WT}*) also rescued the chemotaxis deficit. Chemotaxis tests were also conducted on wild-type worms, *sel-12* mutant worms, and rescue lines over-expressing *Psel-12::PS1_{WT}* in the *sel-12* mutant background at 88, 98, and 108 hours of age (S3 Fig). For each age, *Psel-12::PS1_{WT}* rescue lines restored chemotaxis deficits in *sel-12(ok2078)* mutant worms and had CI values significantly different from *sel-12* mutant worms (At 88 hours [$F(2,17) = 67.98$,

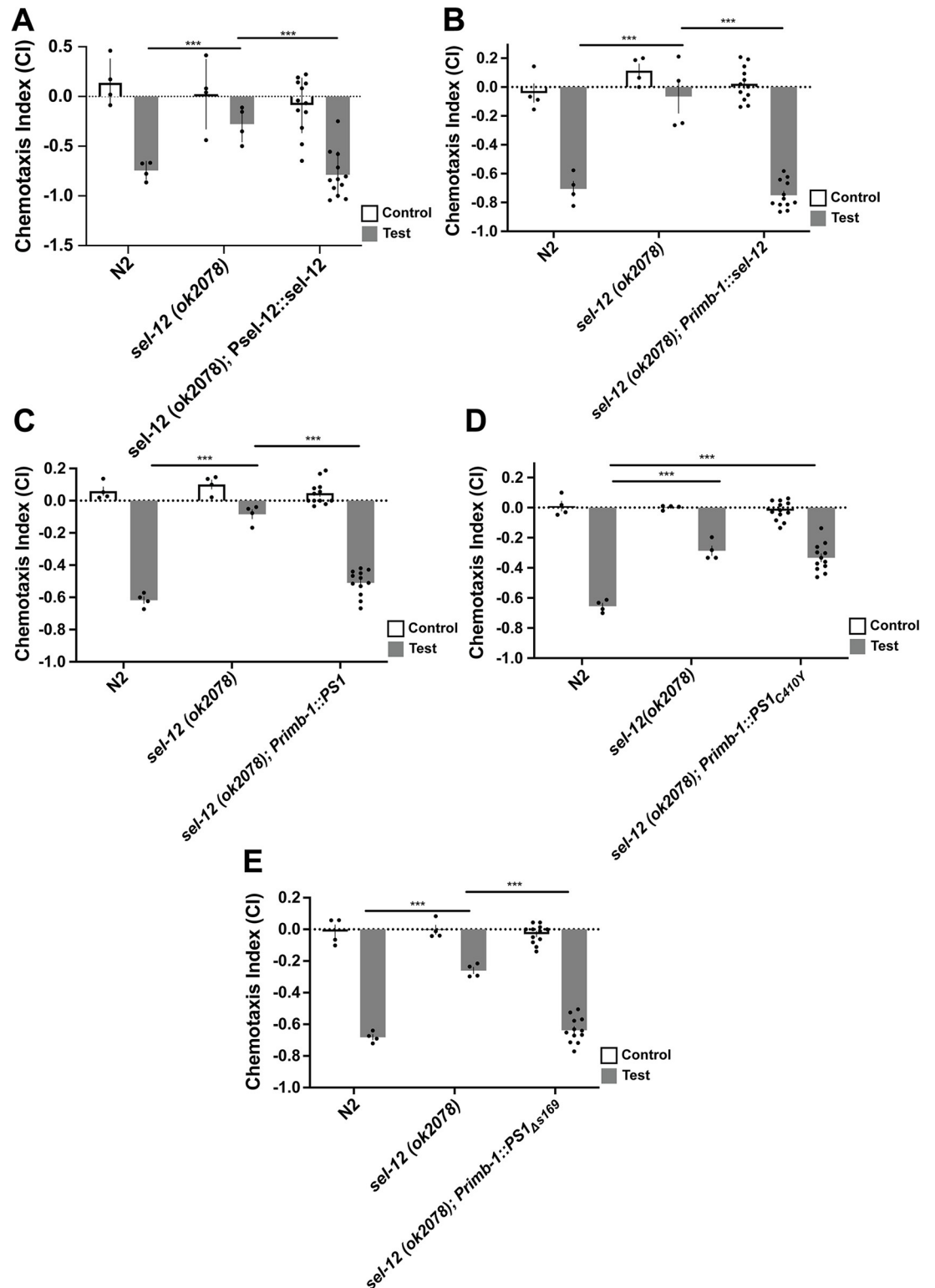


Fig 2. *Psel-12*-driven expression of human wildtype PS1 and pan-neuronal expression of wildtype genes and *PS1_{ΔS169}* rescued octanol chemotaxis deficits in *sel-12* mutant worms. A) *Psel-12::sel-12* rescued chemotaxis deficits of *sel-12* mutants. B) *Primb-1::sel-12* rescued chemotaxis deficits. C) *Ptag-168::PS1* rescued chemotaxis deficits. D) *Ptag-168::PS1_{C410Y}* did not rescue chemotaxis deficits. E) *Ptag-168::PS1_{ΔS169}* rescued chemotaxis deficits. Octanol was used for test (aversive odorant) and M9 for controls (odorless buffer). Each bar represents an average of 4 independent plates (n = 50–100 synchronized 72 hr post

egg-lay young adult worms per plate). Rescue bars are collapsed averages of 3 independent rescue lines generated. Independent plate CI are shown as circles. White bars represent control plates and black bars represent test plates. Error bars reflect the standard error of the mean. *** $p < 0.001$.

<https://doi.org/10.1371/journal.pone.0289435.g002>

$p < 0.001$], at 98 hours [$F(2,17) = 33.92$, $p < 0.001$], and at 108 hours [$F(2,17) = 64.73$, $p < 0.001$]). This finding was consistent with a previous study testing functional conservation between *sel-12* and PS1 in which over-expressing human wild-type PS1 using the endogenous *sel-12* promoter in a *sel-12* mutant rescued mutant phenotypes [30]. Because *sel-12* is expressed in both neuronal and non-neuronal cells in the worm, we next tested whether the octanol chemotaxis deficit could be rescued by expressing PS1 in just the nervous system.

Nervous system expression of wild-type *sel-12*, wild-type PS1, and $PS1_{\Delta s169}$, but not $PS1_{C410Y}$, rescued chemotaxis deficits in *sel-12* mutant worms

In these experiments we used *rimb-1* (formerly *tag-168*), which encodes a pan-neuronally expressed presynaptic active-zone protein [53], to over-express extrachromosomal arrays of wild-type *sel-12*, wild-type PS1, and $PS1_{\Delta s169}$, and $PS1_{C410Y}$, pan-neuronally and tested chemotaxis. *Primb-1::sel-12* rescued the chemotaxis deficits in *sel-12* mutant worms (Fig 2B; [$F(2,17) = 41.68$, $p < 0.001$]; wild-type vs *sel-12* rescue $p = 0.32$, *sel-12* mutant vs *sel-12* rescue $p < 0.001$). Pan-neuronal over-expression of wildtype human PS1 (*Primb-1::PS1_{WT}*) also rescued chemotaxis deficits in *sel-12* mutant worms (Fig 2C; [$F(2,17) = 68.23$, $p < 0.001$]; wild-type vs PS1 rescue $p = 0.44$, *sel-12* mutant vs. PS1 rescue $p < 0.001$).

Interestingly, over-expressing the fAD-linked PS1 mutation C410Y in the nervous system of *sel-12* mutant worms (*Primb-1::PS1_{C410Y}*) did not rescue chemotaxis deficits in *sel-12* mutant worms (Fig 2D; [$F(2,17) = 27.67$, $p < 0.001$]; wild-type vs. $PS1_{C410Y}$ rescue $p < 0.001$, *sel-12* mutant vs. $PS1_{C410Y}$ rescue $p = 0.59$). These findings are also consistent with those of Levitan et al. [30], who showed that fAD-associated PS1 variants were unable to rescue the *sel-12* abnormal vulva and egg-laying phenotypes. Finally, we tested whether the novel fAD-linked mutation, $PS1_{\Delta s169}$, had an effect on chemotaxis. It was previously reported that $PS1_{\Delta s169}$ impacts APP processing and amyloid generation without affecting Notch1 cleavage and Notch signalling as the egg-laying phenotype in *sel-12* worms could be rescued by $PS1_{\Delta s169}$ [38]. Interestingly, in this study over-expressing *Primb-1::PS1_{\Delta s169}* rescued chemotaxis deficits in *sel-12* mutant worms (Fig 2E; [$F(2,17) = 52.24$, $p < 0.001$]; wild-type vs. $PS1_{\Delta s169}$ rescue $p = 0.31$, *sel-12* mutant vs. $PS1_{\Delta s169}$ rescue $p < 0.001$).

In *sel-12* mutant animals an attractive chemotaxis response to diacetyl was also impaired. Using the same strains, we saw that over-expressing *sel-12*, $PS1_{WT}$ and $PS1_{\Delta s169}$ pan-neuronally also rescued impaired diacetyl chemotaxis, while expressing $PS1_{C410Y}$ did not (S4 Fig).

ASH neuron-specific expression of wild-type *sel-12*, wild-type PS1, and $PS1_{\Delta s169}$, but not $PS1_{C410Y}$, rescued chemotaxis deficits in *sel-12* mutant worms

Thus far, our results have aligned with previous studies that show that over-expression of human PS1 in a tissue-specific manner is able rescue phenotypes caused by *sel-12* loss-of-function, suggesting cell-autonomous function [30,51,54]. To take things further, we investigated whether *sel-12* acts in a cell-specific manner through double-dissociation. In *C. elegans*, the ASH sensory neurons are polymodal nociceptors that detect a number of noxious and potentially toxic stimuli including octanol [55]. The avoidance response to octanol is mediated by ASH activation [55]. To determine whether presenilin plays a role in chemotaxis by acting specifically in these sensory neurons, we over-expressed *sel-12*, $PS1_{WT}$, $PS1_{C410Y}$, and $PS1_{\Delta s169}$ in

sel-12(ok2078) mutants driven by promoter region of *sra-6*, a gene strongly expressed in the ASH neurons, and weakly expressed in the ASI neurons and PVQ interneurons [56]. Over-expressing *Psra-6::sel-12* rescued chemotaxis deficits in *sel-12* mutant worms (Fig 3A; [F(2,17) = 45.26, p<0.001]; wild-type vs *sel-12* rescue p = 0.21, *sel-12* mutant vs. *PS1* rescue p<0.001).

Next, we over-expressed wild-type human *PS1* under the control of the *sra-6* promoter (Fig 3B), and found that it rescued the chemotaxis impairments observed in *sel-12* mutant worms

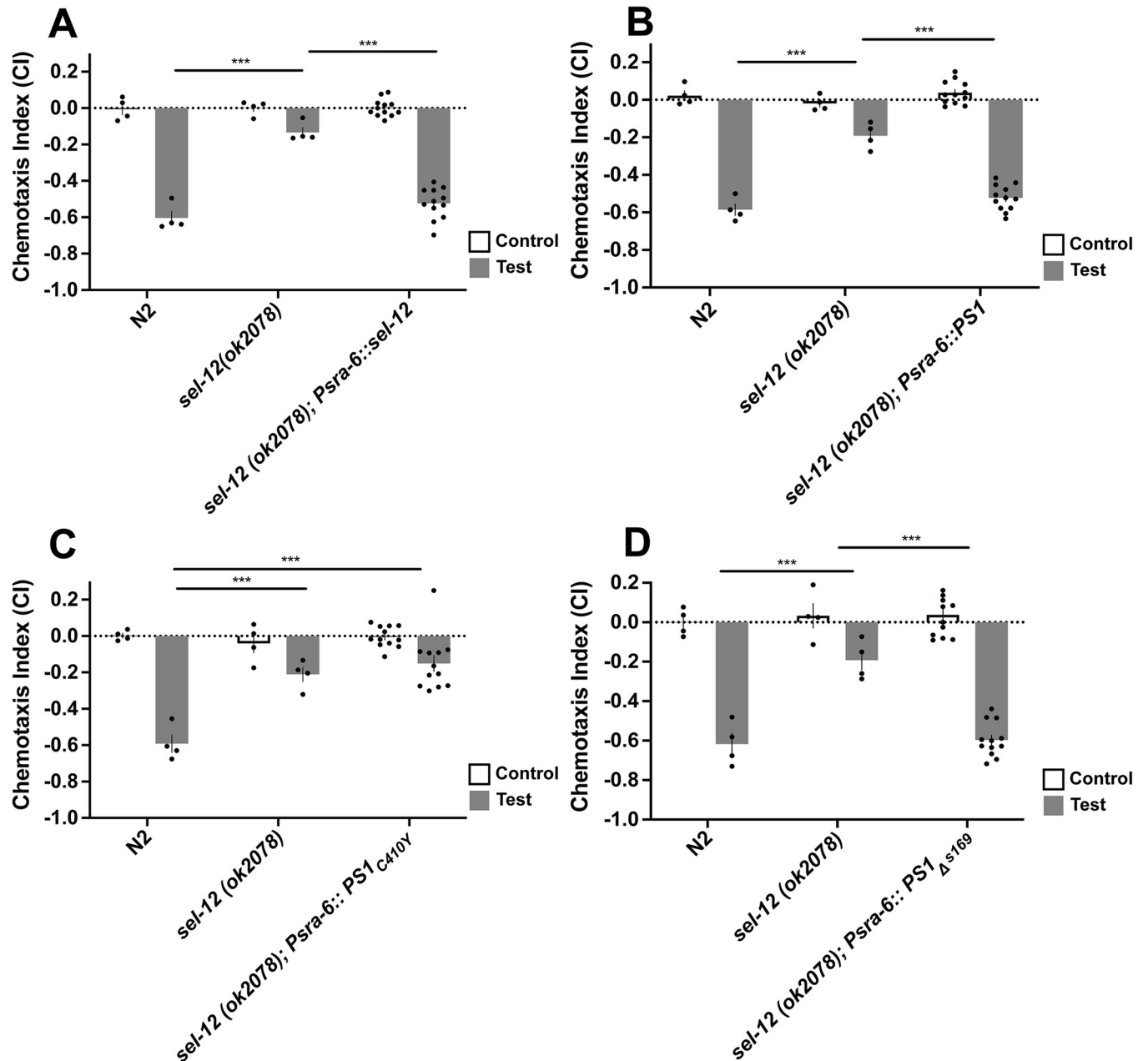


Fig 3. ASH-neuron specific expression of wildtype genes and *PS1^{Δ5169}* rescued octanol chemotaxis deficits in *sel-12* mutant worms. A) *Psra-6::sel-12* rescued chemotaxis deficits. B) *Psra-6::PS1* rescued chemotaxis deficits. C) *Psra-6::PS1^{C410Y}* did not rescue chemotaxis deficits. D) *Psra-6::PS1^{Δ5169}* rescued chemotaxis deficits. Octanol was used for test (aversive odorant) and M9 for controls (odorless buffer). Each bar represents an average from 4 independent plates (n = 50–100 synchronized 72 hr post egg-lay young adult worms per plate). Rescue bars are collapsed averages of 3 independent rescue lines generated. Independent plate CI are shown as circles. White bars represent control plates and black bars represent test plates. Error bars reflect the standard error of the mean. *** p<0.001.

<https://doi.org/10.1371/journal.pone.0289435.g003>

([F(2,17) = 44.29, $p < 0.001$]; wild-type vs $PS1_{WT}$ rescue $p = 0.28$, *sel-12* mutant vs. $PS1$ rescue $p < 0.001$). On the other hand, when we expressed the canonical FAD $PS1$ mutation C410Y in the ASH neurons (*Psra-6::PS1_{C410Y}*; Fig 3C), we found that it did not rescue chemotaxis deficits in *sel-12* mutant worms ([F(2,17) = 16.68, $p < 0.001$]; wild-type vs. $PS1_{C410Y}$ rescue $p < 0.001$, *sel-12* mutant vs. $PS1_{C410Y}$ rescue $p = 0.72$). Finally, in contrast to *Psra-6::PS1_{C410Y}* over-expression, *Psra-6::PS1_{Δs169}* over-expression did restore chemotaxis deficits in *sel-12* mutant worms (Fig 3D; [F(2,17) = 30.69, $p < 0.001$]; wild-type vs. $PS1_{Δs169}$ rescue $p = 0.92$, *sel-12* mutant vs. $PS1_{Δs169}$ rescue $p < 0.001$). This data aligns with previous studies that show that there is functional conservation between human PS1 and its nematode ortholog. The loss-of-function mutations of both PS1 and its nematode ortholog appear to impair cell function in a cell autonomous manner as over-expressing these genes in a single pair of sensory neurons rescued the *sel-12* chemotaxis deficit.

Wild-type $PS1$ rescue lines in the ASH neuron had a cell-specific effect on chemotaxis. Although wild-type $PS1$ in ASH was sufficient to rescue octanol chemotaxis, it is possible that the rescue was not cell-autonomous, and that expression of $PS1_{WT}$ anywhere in the nervous system would rescue the phenotype. To rule out this hypothesis, we expressed wild-type $PS1$ driven by the *odr-10* promoter that is expressed in another pair of chemosensory neurons, the AWA neurons, which are responsible for chemotaxis towards the attractant diacetyl. Consistent with our ASH-octanol avoidance findings, worms with the same mutation in *sel-12* are also deficient in appetitive chemotaxis towards diacetyl and they show the same pattern of chemotaxis deficits and rescues for $PS1_{WT}$ and $PS1$ mutations as was observed for aversive chemotaxis away from octanol (S5A–S5C Fig).

We then tested whether AWA-specific over-expression would rescue ASH-specific phenotypes, and whether ASH-specific over-expression would rescue AWA-specific phenotypes. Over-expression of wild-type $PS1$ in the AWA neurons did not rescue chemotaxis impairment in octanol avoidance (Fig 4A; [F(2,17) = 137.30, $p < 0.001$]; wild-type vs $PS1_{WT}$ rescue $p < 0.001$), but rescued the chemotaxis defect in diacetyl attraction (Fig 4B; [F(2,17) = 100.21, $p < 0.001$]; wild-type vs $PS1_{WT}$ rescue $p = 0.76$). Additionally, over-expressing wild-type $PS1$ in the ASH neurons did not rescue *sel-12* mutant animals' impaired chemotaxis towards diacetyl (Fig 4C; [F(2,17) = 54.00, $p < 0.001$]; wild-type vs $PS1$ rescue $p < 0.001$) but did rescue the chemotaxis away from octanol (Fig 3B).

Thus, expression of $PS1_{WT}$ in the ASH neurons rescued chemotaxis deficits in *sel-12* mutant worms for the octanol odorant, but not for the diacetyl odorant sensed by different sensory neurons, the AWA neurons. At the same time expression of $PS1_{WT}$ in the AWA sensory neurons did not rescue octanol chemotaxis but did rescue chemotaxis to diacetyl. Therefore, via double-dissociation we show that the roles of *sel-12* in mediating the chemotaxis deficits are cell specific, and cell-autonomous.

***C. elegans* with mutations in Notch receptors do not show increased chemotaxis deficits over time**

Contrasting chemotaxis data from animals with the two FAD mutations, the classic mutation $PS1_{C410Y}$ that alters both A β and Notch cleavage, and $PS1_{Δs169}$ mutation that affects A β cleavage but leaves Notch intact, suggested an important role for Notch cleavage by *sel-12* in normal chemotaxis. Like APP, Notch receptors are cleaved and activated by the presenilins of γ -secretase. In earlier research it was reported that in *C. elegans* the two Notch receptors, *lin-12* and *glp-1*, redundantly regulate chemosensory avoidance behavior in response to octanol [57]. As single mutations of either *glp-1* or *lin-12* did not show chemotaxis impairments [57], we used the transgenic strain created by Singh *et al.* in which *glp-1* was knocked down using heat-

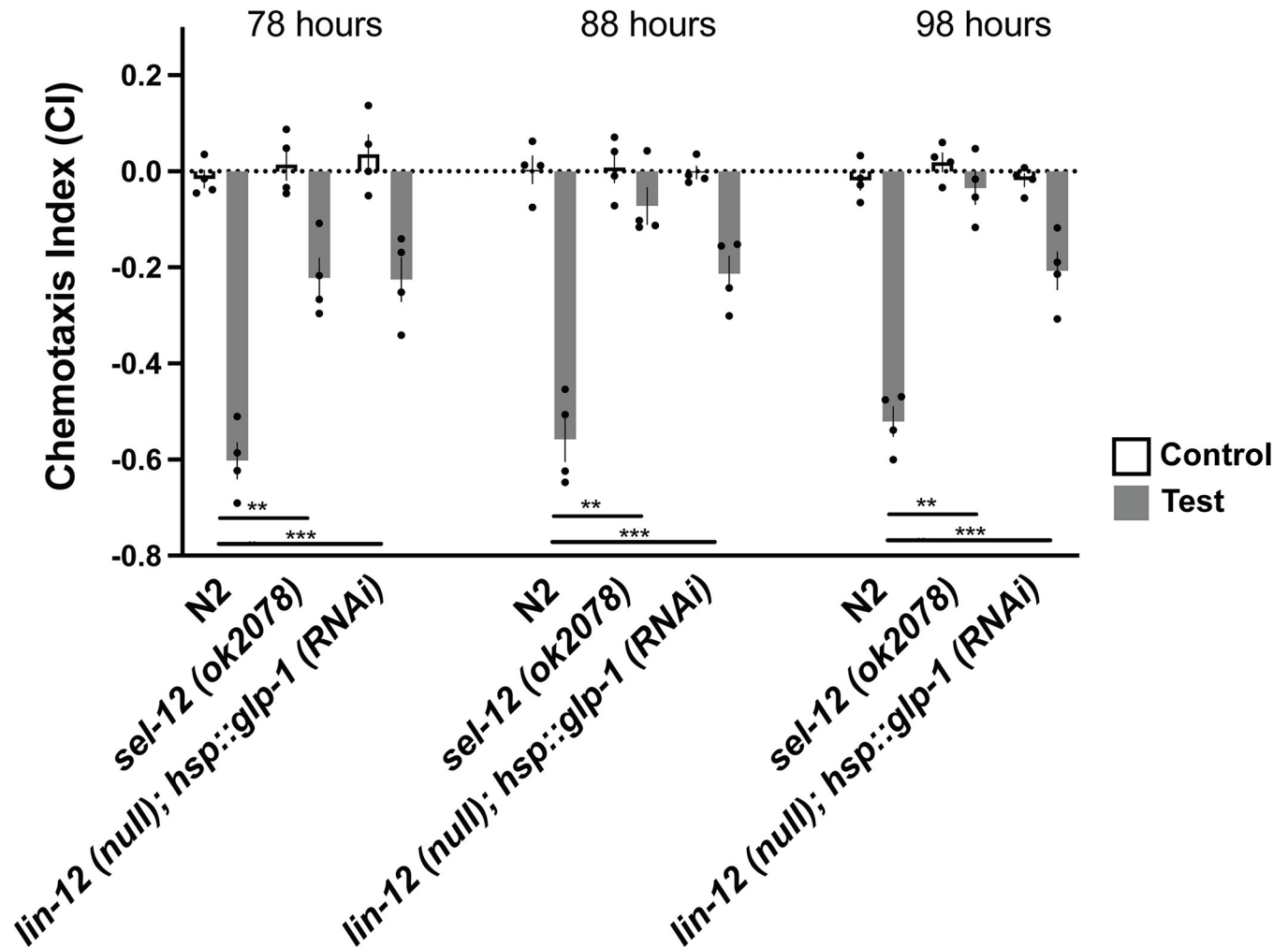


Fig 4. Wildtype *PS1* over-expression in the ASH neuron had a cell-specific effect on rescuing chemotaxis in *sel-12* mutant background. Wildtype *PS1* was expressed in AWA neurons by *odr-10* promoter (responsible for diacetyl) and ASH neurons by *sra-6* promoter (responsible for octanol) cell-specifically. **A)** *Podr-10::PS1* did not rescue chemotaxis deficits in response to octanol. **B)** *Podr-10::PS1* rescued chemotaxis deficits in response to diacetyl. **C)** *Psra6::PS1* did not rescue chemotaxis deficits in response to diacetyl. Bars with a solid outline denote chemotaxis assays done with octanol, while dotted bars denote a chemotaxis assays done with diacetyl. Each bar represents an average from 4 independent plates (n = 50–100 synchronized 72 hr post egg-lay young adult worms per plate). Rescue bars are collapsed averages of 3 independent rescue lines generated. Independent plate CI are shown as circles. White bars represent control plates and black bars represent test plates. Error bars reflect the standard error of the mean. *** p < 0.001.

<https://doi.org/10.1371/journal.pone.0289435.g004>

shock promotor driven RNAi in adult *lin-12(n941)* mutants, and tested octanol chemotaxis of this strain as worms aged to determine whether these deficits increased in the same way as did chemotaxis in the *sel-12* mutant worms.

Both *sel-12* mutant worms and *lin-12/glp-1* mutant worms had significantly lower CIs compared to wild-type worms (p < 0.001; Fig 5). Compared to age-matched wild-type worms, *C. elegans* with *lin-12(n941)/glp-1* reduction-of-function did not show increasingly impaired octanol chemotaxis over time (p = 1.00). This is in contrast with wild-type (N2) and *sel-12* mutant worms that demonstrated an increase in chemotaxis deficits over time (p < 0.001). These findings suggest that Notch associated chemotaxis deficits do not fully phenocopy all of the characteristics of mutations in *sel-12*.

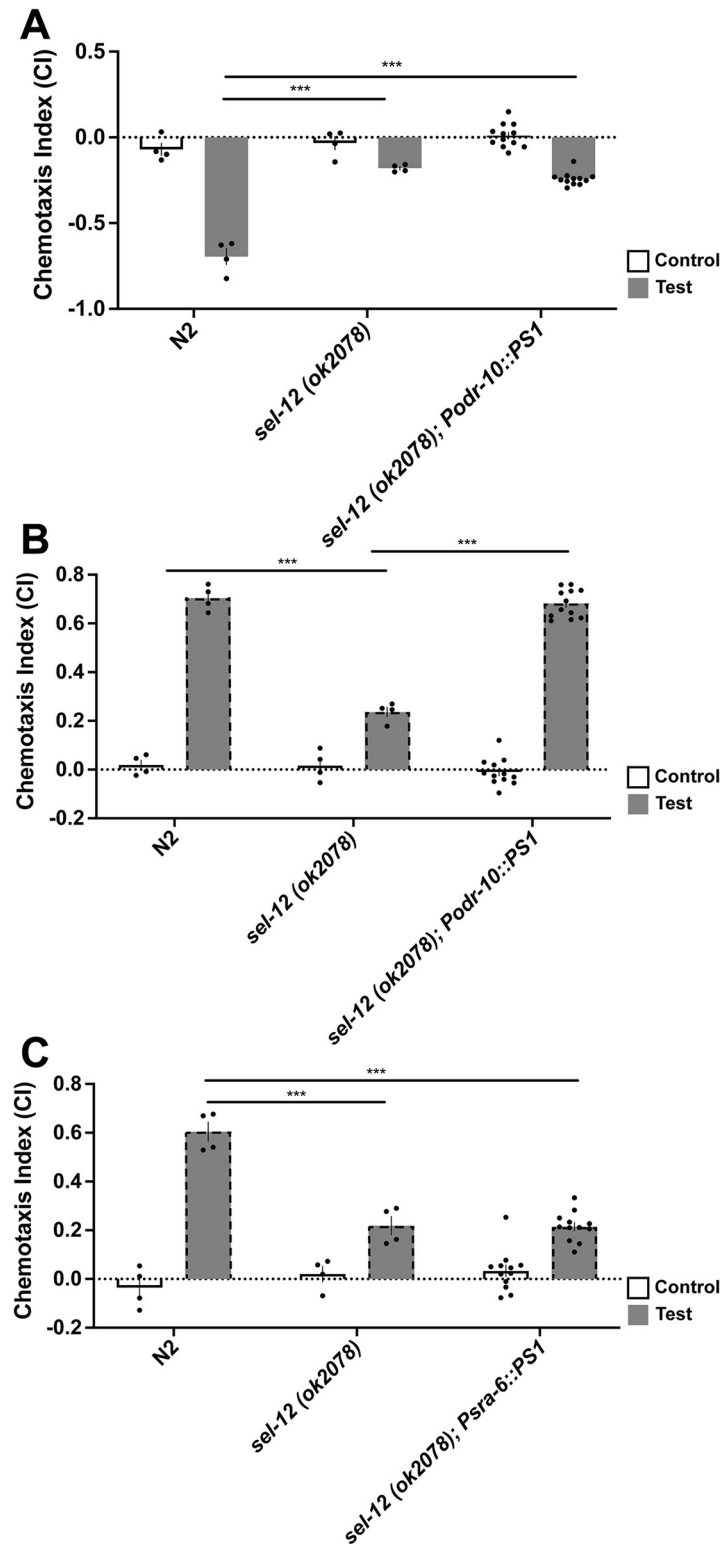


Fig 5. Worms with RNAi knockdown of *glp-1* in a *lin-12* null background showed chemotaxis deficits that did not progress over time. Octanol was used for test (aversive odorant) and M9 for controls (odorless buffer). Each bar represents an average from 4 independent plates (n = 50–100 synchronized 72 hr post egg-lay young adult worms per plate). Independent plate CI are shown as circles. White bars represent control plates and black bars represent test plates. Error bars reflect the standard error of the mean. *** p<0.001.

<https://doi.org/10.1371/journal.pone.0289435.g005>

sel-12* mutant *C. elegans* have ASH neuron morphological abnormalities that are rescued by wild-type *PSI* and *PSI_{Δs169}*, but not *PSI_{C410Y}

The chemotaxis experiments showed that *sel-12* mutant worms had chemotaxis deficits that increased as worms aged. What causes the chemotaxis deficits? Since neuronal death is observed in AD we hypothesized that there might be neuronal degeneration occurring in *sel-12* worms. This led us to investigate whether the chemotaxis behavioral phenotype reflected morphological changes or neurodegeneration of the sensory neurons. Inspired by results from past studies that showed that *sel-12* loss-of-function mutants cause morphology defects in neurons corresponding to thermotaxis [51] and mechano-sensation [58] that aligned with observed behavioural phenotypes, we sought to study morphology of the ASH neurons what mediate our studied chemotaxis behaviour. To address whether the loss-of-function mutation in *sel-12* altered the morphology of the ASH neurons, we crossed the *sel-12(ok2078)* mutant into a strain of worms expressing cytosolic GFP in the ASH neurons (*osm-10::GFP*), and using this resultant strain as the background generated transgenic lines over-expressing *PSI_{WT}*, *PSI_{Δs169}* and *PSI_{C410Y}*. Using a confocal microscope we imaged the ASH neurons in separate groups of 100 wild-type, *sel-12* mutant, *Psra-6::PSI_{WT}*, *Psra-6::PSI_{Δs169}*, and *Psra-6::PSI_{C410Y}* worms at 78, 98, and 108 hours of age. Observed neuron morphologies were categorized into “normal”, “gapped”, or “blebs” (Fig 6A). When we visualized the same GFP-filled ASH neurons using a DiI dye-filling protocol [59], the GFP co-localized with DiI dye, suggesting that the blebbing and gap phenotypes observed are indeed indicative of degenerated processes and not due to punctate or non-uniform distribution of GFP (Fig 6B). Within the same strain, there appeared to be no significant differences in the total number of abnormal ASH neurons

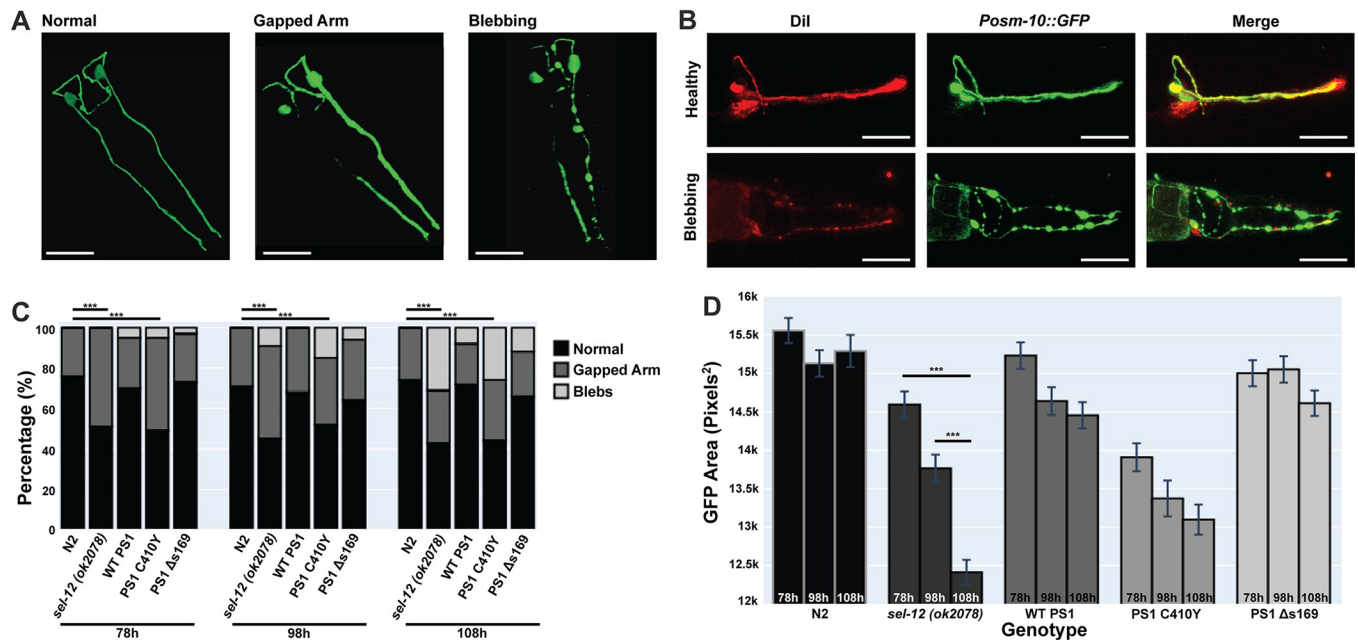


Fig 6. *sel-12* mutant worms have impaired ASH sensory neuron morphology that was rescued by ASH-specific expression of wild-type and *PSI_{Δs169}*. A) Categories of ASH sensory neuron morphology. ASH neurons have been categorized as healthy with normal morphology, having gaps in the processes or have circular blebs. Both gaps and blebs are indicative of neurodegeneration. Scale bar = 30µm B) In healthy ASH neurons, dye-fill with DiI overlaps with *Posm-10::GFP*. In degenerating ASH neurons, there is little or no overlap between DiI dye-fill and the fluorescent marker. Scale bar = 30µm. C) ASH neuron morphology of five strains (n = 100 per strain per time point) over time (78, 98, and 108 hour old worms). Different worms were used for each time point. ASH neurons of wildtype, *sel-12* mutant, ASH-specific wildtype *PSI* rescues, ASH-specific *PSI_{Δs169}* rescues, and ASH-specific *PSI_{C410Y}* rescues were imaged and categorized as either normal or abnormal (gapped arm or blebs). $\chi^2(1, N = 200) = 16.33, p < 0.01$. D) ASH GFP area quantification in pixels². *** p < 0.001.

<https://doi.org/10.1371/journal.pone.0289435.g006>

across different ages (Fig 6C; $p > 0.05$ between all ages within the same strains). A chi-square test showed that *sel-12* worms had significantly fewer normal ASH neurons compared to wild-type worms across all time points, $X^2(1, N = 200) = 16.33, p < 0.01$. However, as worms aged there appeared to be a progression from a “gapped arm” state to a more severe “blebbed” state in degenerating neurons—and this progression appeared more prominent in *sel-12* mutants and $PS1_{C410Y}$ over-expression animals. Animals with ASH neuron-specific expression of wild-type *PS1* and $PS1_{\Delta s169}$, had significantly more normal neurons than *sel-12* animals and were not significantly different from wild-type, however animals with $PS1_{C410Y}$ were not significantly different from *sel-12* animals and had significantly fewer normal neurons than wild-type animals (Fig 6C). As a proxy measure for the health of the neurons the area of GFP in each neuron was quantified. ASH neurons in wild-type worms had significantly larger GFP area compared to *sel-12* mutant worms at all time points; in *sel-12* mutant animals the decrease in GFP area across age is particularly noticeable (Fig 6D). These data support the hypothesis that in *sel-12* mutants the ASH neurons were degenerating as worms aged. This observed phenotype is rescued by human Wildtype *PS1* and $PS1_{\Delta s169}$ over-expression but not $PS1_{C410Y}$.

Discussion

Our studies expand on previous evidence supporting the hypothesis of an $A\beta$ -independent role of human *PS1* in neural degeneration by studying *sel-12*, the *C. elegans* orthologue of *PS1*, *in vivo*. We demonstrated that in an $A\beta$ -absent model, C410Y mutations in *PS1* lead to AD-like pathogenesis and neuronal dysfunction in a cell-specific and cell-autonomous manner, whereas the Notch-intact $\Delta s169$ mutation largely rescues *sel-12* mutant phenotypes. Importantly, expanding on previous studies that have alluded to the cell-autonomous function *sel-12* [30,51,54], we demonstrate that the role of *sel-12* in mediating chemotaxis acts in a cell-specific and cell-autonomous manner through double-dissociation (Figs 3 and 4, S5 Fig).

We observed that worms with *sel-12* mutations had chemotaxis deficits from shortly after hatching, and that these deficits increased with age (Fig 1D). The ASH neurons that are responsible for detection of the octanol odorant showed morphological abnormalities indicative of neurodegeneration and degenerated more rapidly in *sel-12* mutant worms compared to wild-type worms (Fig 6). This progressive neurodegeneration paralleled the decline of the chemotaxis indices of *sel-12* mutant worms over time. Human *PS1* and *sel-12* have considerable conservation of function, such that the over-expression of human WT *PS1* rescued *sel-12* mutant phenotypes [30]. Consistent with past findings, here we found that the over-expression of either wild-type *sel-12* or human *PS1* in the ASH neurons rescued both chemotaxis deficits and ASH morphological abnormalities in *sel-12* mutant worms (Figs 2 & 6).

Because *sel-12* is strongly expressed in all *C. elegans* neurons, these data raise the question of whether the entire nervous system degenerates as a result of *sel-12* mutations. Our behavioural data suggest that, in addition to the ASH neurons, the AWA sensory neurons may also be degenerating. Previous work on *sel-12* worms examined the AIY interneurons and the mechanosensory neurons (ALM and PLM). Wittenburg *et al.* [51] showed that *C. elegans* with mutations in *sel-12* have defects in thermotaxis behaviour as a result of a loss of function in cholinergic interneurons from the time of hatching [51]. They also showed that these mutant worms displayed abnormal morphologies in the AIY interneurons, and that this phenotype was rescued by AIY-specific wild-type *sel-12* and wild-type *PS1* expression [51]. Sarasija *et al.* [58] reported that mutations in *sel-12* lead to metabolic defects of the mitochondria, resulting in oxidative stress and neurodegeneration in the ALM and PLM neurons responsible for responding to mechanical stimuli [58]. Reducing calcium levels in the mitochondria in *sel-12* mutant worms prevented neurodegeneration in mechanosensory neurons [58]. Therefore, it is

possible that mutations in *sel-12* impact a number of neurons. Our locomotion data suggests that not all neurons are affected in mature *sel-12* mutant worms as they were still able to move about on the agar surface, indicating that the motor neurons continue to drive movement even in the oldest worms we tested (S2A and S2B Fig). *C. elegans* provides a unique system in which the role of presenilin in olfactory dysfunction and neuron death can be investigated using single cell rescues. As presenilins are substrates for different caspase proteins, the interaction between *PS1* and caspases can be further explored. This use of single cell resolution phenotyping allows the characterization of even subtle and pleiotropic phenotypes, providing potential novel therapeutic opportunities.

While findings from our experiments are consistent with other observations in the literature that demonstrate mechanistic loss-of-function phenotypes of PS1 function, our experiments do not reconcile this with the autosomal dominant nature of pathogenic PS mutations in *fAD*. In our experiments transgenes were over-expressed as extrachromosomal arrays leading to variability between the transgenic lines. We do not know the copy number of the transgenes expressed by these arrays (it could be a few copies or several hundred copies), and the expression level would likely have been much higher than what is found *in vivo*. This suggests to us that overexpressed levels of wildtype *sel-12* and human PS1 do not cause any deficits in chemotaxis in *C. elegans*. Newer techniques such as the Mos10 mediated Single Copy Insertion (MosSCI) [60] and the CRISPR-Cas9 system can be used in *C. elegans* to generate single or low number copy rescues [61]. Both approaches would allow a single copy of PS1 to replace mutant *sel-12* in worms and might produce more consistent effects. Additionally, this approach can make testing phenotypes in a heterozygote possible and further resolve the paradox between the mechanistic loss-of-function hypothesis of PS and the autosomal dominant mode nature of pathogenic mutations of PS. Interestingly, in mice studies inactivation of a single PS1 locus is not sufficient to cause neurodegeneration while having one copy of a pathogenic variant is [62,63]—it is hypothesized, therefore, that the resulting mutant protein is antimorphic and in addition to being loss-of-function can act in a dominant-negative manner to inhibit the activities of normal PS produced from the remaining alleles to cause the dominant inheritance pattern of PS mutations. This hypothesis has yet to be fully explored.

This work together with previous studies [58,64] demonstrate that neurodegeneration of neurons in *C. elegans* with *sel-12* mutations can occur in the absence of A β deposits. This offers an opportunity to study the role presenilins may play in neurodegeneration, independent of A β . While previous work suggested that the *sel-12* neural degeneration was due to a Notch-independent mitochondrial dysfunction pathway [58], redundancy of function between *glp-1* and *lin-12* was not tested in these experiments. Our data suggests that although Notch contributes to the chemotaxis deficit phenotypes, double loss or knock-down of Notch receptors shows that the age-progressive phenomenon may be Notch-independent.

Perhaps the most interesting observation from our experiments was that whereas overexpression of human *PS1*_{C410Y} did not rescue *sel-12* loss-of-function deficits, over-expression of the *PS1* _{Δ S169} variant rescued both the chemotaxis and neurodegeneration phenotypes. As *PS1* _{Δ S169} is hypothesized not to affect Notch signaling while *PS1*_{C410Y} does, and that *PS1* _{Δ S169} rescued both the chemotaxis and neurodegeneration phenotypes observed in our studies, it may be that Notch is an important signaling pathway for AD pathology. Indeed, the fact that decreased expression of both of the two Notch receptors *lin-12* and *glp-1* together exhibited chemotaxis deficits suggests that the phenotypes observed in this study are predominantly linked to Notch signalling [45]. Indeed, Notch1 activation and expression has been shown to be significantly reduced in neurons in brain tissue and from AD patients [65] and altered Notch regulation can contribute to pathology of disease. Therefore, we investigated whether the interaction between *PS1* and Notch played a role in these chemotaxis deficits by knocking

down *glp-1* with RNAi in a *lin-12* mutant strain and confirmed the importance of Notch for the chemotaxis phenotype. Our data with PS1 $_{\Delta s169}$ and the Notch knockdown experiments appears to suggest that in the *C. elegans* model the deficits caused by *sel-12* loss-of-function and PS1 $_{C410Y}$ are derived largely from Notch signalling, which is contrary to the fact that the patient mutation PS1 $_{\Delta s169}$ itself is a pathogenic variant. This could possibly be explained by *C. elegans* lacking a mammalian ortholog for APP and β -secretase that induce deleterious effects in mechanisms that are present in the mammalian system [29]. However, we also found that the chemotaxis deficits induced by impairments in Notch signaling did not increase as animals aged (Fig 4). This suggests that although Notch plays an important role in octanol chemotaxis, the age-dependent and progressive component of the behavioural deficits we observed may be mediated by another Notch-independent pathway that *sel-12/PS1* regulates.

To further examine whether the chemotaxis deficits and neurodegeneration we observed in our experiments are purely due to Notch or do indeed have a Notch-independent component, a more detailed analysis—including studying a *sel-12;lin-12;glp-1* triple knockdown for both chemotaxis and neurodegeneration phenotypes to parse out an epistatic relationship between *sel-12* and the Notch receptors—is required. However, the *sel-12* strain and the *lin-12;glp-1* strain used in this study are problematic to cross because hermaphrodites of both strains display the bag-of-worm phenotype due to improper development of vulval tissue [41,66] and males of both strains have significant mating deficiencies because of developmental defects in the male sex tissues [67,68]. Additionally, the *hsp::glp-1* RNAi construct is overexpressed as an extrachromosomal array and the mosaic inheritance enhances the difficulty in generating and selecting transgenic males across generations for a cross. As a result, we were not successful in generating a triple mutant as suggested above to further elaborate the involvement of Notch in our phenotypes.

It is also possible that loss of SEL-12/PS1 may cause some components of our observed phenotype through a Notch-independent and Amyloid-independent mechanism. Indeed, presenilin loss has been found to cause Ca²⁺ mediated mitochondrial dysfunction to drive neurodegeneration [54,58]. Whether mitochondrial dysfunction, or another mechanism yet to be found, may mediate the phenotypes we observe in the *sel-12* mutant and human PS1 over-expression strains would be an exciting direction to follow-up on. Studies interrogating other molecular pathways PS1 is involved in will uncover possible other pathways of PS1 that may contribute to fAD.

From the perspective of neurodegeneration the results we obtained can best be explained by two possibilities: one, that the fAD mutation has a lethal effect in neurons leading to cell death, or two, that presenilins play an important role in cell maintenance or survival and that classic fAD mutations interfere with that function and without it neurons die. Thus, a pathogenic mutation either kills the cell, or stops an essential function required for the cell to survive. This offers interesting research questions to pursue in the future. Our observation of cell-specific rescue shows that the effect of the mutation is cell specific and so is not a circuit issue, but an issue at the level of individual neurons. Loss-of-function of *sel-12* has been linked to autophagy-mediated neurodegeneration in *C. elegans* [64], but more research is required to elucidate the roles other cell-death pathways may play in *sel-12* mediated neurodegeneration as well. *C. elegans* offers the unique opportunity to study the functions of human disease genes and disease-causing mutations at the level of single neurons in living, behaving animals. This knowledge may lead to novel approaches to studying AD and developing new approaches to diagnosis and treatment of this debilitating disorder.

Supporting information

S1 Table. List of all strains generated and tested.
(CSV)

S1 Fig. Amino acid sequence of human PS1 and its *C. elegans* orthologs *HOP-1* and *SEL-12*. MUSCLE (Multiple Sequence Comparison by Log-Expectation) from the EMBL's European Bioinformatics Institute Job Dispatcher (www.ebi.ac.uk/jdispatcher/msa) was used to generate multiple sequence alignment. Highlighted residues (red) are locations of known pathogenic or likely pathogenic variants of PS1. The two variants investigated in this study is highlighted in a different color (green). Amino acids that are identical between human PS1 and its *C. elegans* orthologs are or also highlighted (purple) in each respective sequence. (TIF)

S2 Fig. Locomotion is reduced but is not abolished to impact chemotaxis in *sel-12* mutant worms. A) Average forward movement speed of 68–108 hour old wild-type and *sel-12* mutant worms. Blue bars and red bars represent wild-type (N2) and *sel-12* mutant worms, respectively. Each bar represents an average from 3 independent plates (n = 50 worms per plate). LOF: Loss of function. Error bars reflect the standard error of the mean. B) locomotion tracks of 88 to 108 hour old wild-type, *sel-12* mutant, and nervous system *PS1* rescue worms over a 250 second tracking period. Different colors indicate various tracking time points after a brief air-puff. (n = 50 worms per plate). One representative line is shown for the rescue experiment, as all three extrachromosomal lines followed the same trend. ** P<0.01. (TIF)

S3 Fig. *Psel-12::PS1* rescued chemotaxis deficits of *sel-12* across 88, 98 and 108 hours of age. Octanol was used for test (aversive odorant) and M9 for controls (odorless buffer). Each bar represents an average of 4 independent plates (n = 50–100 worms per plate). Rescue bars are collapsed averages of 3 independent rescue lines generated. Independent plate CI are shown as circles. White bars represent control plates and black bars represent test plates. Error bars reflect the standard error of the mean. *** p<0.001. (TIF)

S4 Fig. Endogenous and pan-neuronal and expression of wildtype genes and *PS1_{Δs169}* rescued diacetyl chemotaxis deficits in *sel-12* mutant worms. *Psel-12::sel-12* (A), *Primb-1::sel-12* (B), *Primb-1::PS1* (C), and *Primb-1::PS1_{Δs129}* (E) rescued chemotaxis deficits on diacetyl, whereas *Primb-1::PS1_{C410Y}* (D) did not. Diacetyl was used for test (attractive odorant) and M9 for control (odorless buffer). Independent plate CIs are shown as circles. Each bar represents and average from 4 independent plates (n = 50–100 synchronized 72 hr post egg-lay young adult worms per plate). Rescue bars are collapsed averages of 3 independent rescue lines generated. White bars represent control plates and black bars represent test plates. Error bars reflect the standard error of the mean. *** p<0.001. (TIF)

S5 Fig. AWA-specific expression of wildtype genes and *PS1_{Δs169}* rescued diacetyl chemotaxis deficits in *sel-12* mutant worms. *Podr-10::sel-12* (A) and *Podr-10::PS1_{Δs169}* (C) rescued chemotaxis deficits to diacetyl, whereas *Podr-10::PS1_{C410Y}* (B) did not. Diacetyl was used for test (attractive odorant) and M9 for control (odorless buffer). Independent plate CI are shown as circles. Each bar represents an average from 4 independent plates (n = 50–100 synchronized 72 hr post egg-lay young adult worms per plate). Rescue bars are collapsed averages of 3 independent rescue lines generated. White bars represent control plates and black bars represent test plates. Error bars reflect the standard error of the mean. *** p<0.001. (TIF)

Acknowledgments

The authors would like to thank the Caenorhabditis Genetics Centre (CGC) for providing the wild-type and *sel-12* mutant strains, Dr. Ann Hart for providing the Notch mutant strains, Dr. Ralf Baumeister for providing the wild-type *sel-12*, *PSI*, and *PSI_{C410Y}* strains, and Dr. Weihong Song for providing the *PSI_{Δs169}* plasmid. In addition, we thank Dr. Anne Hart and Dr. Ken Norman for advice and feedback regarding generating a proposed triple mutant.

Author Contributions

Conceptualization: Mahraz Parvand, Tahereh Bozorgmehr, Catharine H. Rankin.

Data curation: Mahraz Parvand, Joseph J. H. Liang.

Formal analysis: Mahraz Parvand, Joseph J. H. Liang.

Funding acquisition: Catharine H. Rankin.

Investigation: Mahraz Parvand, Joseph J. H. Liang.

Methodology: Mahraz Parvand, Joseph J. H. Liang, Tahereh Bozorgmehr, Dawson Born, Alvaro Luna Cortes.

Resources: Catharine H. Rankin.

Supervision: Mahraz Parvand, Alvaro Luna Cortes, Catharine H. Rankin.

Visualization: Joseph J. H. Liang.

Writing – original draft: Mahraz Parvand.

Writing – review & editing: Joseph J. H. Liang, Catharine H. Rankin.

References

1. Qiu C, Kivipelto M, Von Strauss E. Epidemiology of Alzheimer's disease: Occurrence, determinants, and strategies toward intervention. Vol. 11, *Dialogues in Clinical Neuroscience*. 2009. p. 111–28. <https://doi.org/10.31887/DCNS.2009.11.2/cqiu> PMID: 19585947
2. Montine TJ, Koroshetz WJ, Babcock D, Dickson DW, Galpern WR, Maria Glymour M, et al. Recommendations of the alzheimer's disease-related dementias conference. *Neurology*. 2014; 83(9):851–60. <https://doi.org/10.1212/WNL.0000000000000733> PMID: 25080517
3. Lista S, O'Bryant SE, Blennow K, Dubois B, Hugon J, Zetterberg H, et al. Biomarkers in Sporadic and Familial Alzheimer's Disease. Vol. 47, *Journal of Alzheimer's Disease*. 2015. p. 291–317. <https://doi.org/10.3233/JAD-143006> PMID: 26401553
4. Bertram L, Tanzi RE. The genetics of Alzheimer's disease. In: *Progress in Molecular Biology and Translational Science*. 2012. p. 79–100. <https://doi.org/10.1016/B978-0-12-385883-2.00008-4> PMID: 22482448
5. Bateman RJ, Xiong C, Benzinger TLS, Fagan AM, Goate A, Fox NC, et al. Clinical and Biomarker Changes in Dominantly Inherited Alzheimer's Disease. *N Engl J Med*. 2012/07/11 ed. 2012 Aug; 367(9):795–804. <https://doi.org/10.1056/NEJMoa1202753> PMID: 22784036
6. De Strooper B, Iwatsubo T, Wolfe MS. Presenilins and γ -secretase: Structure, function, and role in Alzheimer disease. *Cold Spring Harb Perspect Med*. 2012 Jan; 2(1):a006304–a006304.
7. Alzforum. Mutations Database [Internet]. 2022 [cited 2022 Aug 22]. Available from: <http://www.alzforum.org/mutations>
8. Levy-Lahad E, Wasco W, Poorkaj P, Romano DM, Oshima J, Pettingell WH, et al. Candidate gene for the chromosome 1 familial Alzheimer's disease locus. *Science*. 1995 Aug; 269(5226):973–7. <https://doi.org/10.1126/science.7638622> PMID: 7638622
9. Bergmans BA, De Strooper B. γ -secretases: from cell biology to therapeutic strategies. Vol. 9, *The Lancet Neurology*. England; 2010. p. 215–26.
10. Sun L, Zhou R, Yang G, Shi Y. Analysis of 138 pathogenic mutations in presenilin-1 on the in vitro production of A β 42 and A β 40 peptides by γ -secretase. *Proc Natl Acad Sci U S A*. 2017; 114(4):E476–85.

11. Hardy JA, Higgins GA. Alzheimer's Disease: The Amyloid Cascade Hypothesis. *Science*. 1992; 256:184–5. <https://doi.org/10.1126/science.1566067> PMID: 1566067
12. Jagust W. Is amyloid- β harmful to the brain? Insights from human imaging studies. *Brain*. 2016; 139(1):23–30.
13. Herrup K. Reimagining Alzheimer's disease—An age-based hypothesis. Vol. 30, *Journal of Neuroscience*. 2010. p. 16755–62. <https://doi.org/10.1523/JNEUROSCI.4521-10.2010> PMID: 21159946
14. Esquerda-Canals G, Montoliu-Gaya L, Güell-Bosch J, Villegas S. Mouse Models of Alzheimer's Disease. *J Alzheimers Dis*. 2017 Apr 19; 57(4):1171–83. <https://doi.org/10.3233/JAD-170045> PMID: 28304309
15. Elder GA, Gama Sosa MA, De Gasperi R. Transgenic Mouse Models of Alzheimer's Disease. *Mt Sinai J Med J Transl Pers Med*. 2010 Jan; 77(1):69–81. <https://doi.org/10.1002/msj.20159> PMID: 20101721
16. Elder GA, Gama Sosa MA, De Gasperi R, Dickstein DL, Hof PR. Presenilin transgenic mice as models of Alzheimer's disease. *Brain Struct Funct*. 2010 Mar 18; 214(2–3):127–43. <https://doi.org/10.1007/s00429-009-0227-3> PMID: 19921519
17. Watanabe H, Iqbal M, Zheng J, Wines-Samuels M, Shen J. Partial loss of presenilin impairs age-dependent neuronal survival in the cerebral cortex. *J Neurosci*. 2014; 34(48):15912–22. <https://doi.org/10.1523/JNEUROSCI.3261-14.2014> PMID: 25429133
18. Kang J, Shen J. Cell-autonomous role of Presenilin in age-dependent survival of cortical interneurons. *Mol Neurodegener*. 2020; 15(1):1–17.
19. Saura CA, Choi SY, Beglopoulos V, Malkani S, Zhang D, Shankaranarayana Rao BS, et al. Loss of presenilin function causes impairments of memory and synaptic plasticity followed by age-dependent neurodegeneration. *Neuron*. 2004 Apr 8; 42(1):23–36. [https://doi.org/10.1016/s0896-6273\(04\)00182-5](https://doi.org/10.1016/s0896-6273(04)00182-5) PMID: 15066262
20. Chui DH, Tanahashi H, Ozawa K, Ikeda S, Checler F, Ueda O, et al. Transgenic mice with Alzheimer presenilin 1 mutations show accelerated neurodegeneration without amyloid plaque formation. *Nat Med*. 1999 May 1; 5(5):560–4. <https://doi.org/10.1038/8438> PMID: 10229234
21. Zaman SH, Parent A, Laskey A, Lee MK, Borchelt DR, Sisodia SS, et al. Enhanced Synaptic Potentiation in Transgenic Mice Expressing presenilin 1 Familial Alzheimer's Disease Mutation Is Normalized with a Benzodiazepine. *Neurobiol Dis*. 2000 Feb; 7(1):54–63. <https://doi.org/10.1006/nbdi.1999.0271> PMID: 10671322
22. Shen J, Kelleher RJ. The presenilin hypothesis of Alzheimer's disease: Evidence for a loss-of-function pathogenic mechanism. *Proc Natl Acad Sci*. 2007 Jan 9; 104(2):403–9. <https://doi.org/10.1073/pnas.0608332104> PMID: 17197420
23. Artavanis-Tsakonas S, Matsuno K, Fortini ME. Notch signaling. *Science*. 1995 Apr; 268(5208):225–32. <https://doi.org/10.1126/science.7716513> PMID: 7716513
24. Kopan R, Schroeter EH, Weintraub H, Nye JS. Signal transduction by activated mNotch: Importance of proteolytic processing and its regulation by the extracellular domain. *Proc Natl Acad Sci U S A*. 1996 Feb; 93(4):1683–8. <https://doi.org/10.1073/pnas.93.4.1683> PMID: 8643690
25. Louvi A, Artavanis-Tsakonas S. Notch signalling in vertebrate neural development. Vol. 7, *Nature Reviews Neuroscience*. England; 2006. p. 93–102. <https://doi.org/10.1038/nrn1847> PMID: 16429119
26. Berezovska O, Xia MQ, Hyman BT. Notch is expressed in adult brain, is coexpressed with presenilin-1, and is altered in Alzheimer disease. *J Neuropathol Exp Neurol*. 1998; 57(8):738–45. <https://doi.org/10.1097/00005072-199808000-00003> PMID: 9720489
27. Costa RM, Honjo T, Silva AJ. Learning and memory deficits in notch mutant mice. *Curr Biol*. 2003; 13(15):1348–54. [https://doi.org/10.1016/s0960-9822\(03\)00492-5](https://doi.org/10.1016/s0960-9822(03)00492-5) PMID: 12906797
28. Woo HN, Park JS, Gwon AR, Arumugam T V., Jo DG. Alzheimer's disease and Notch signaling. Vol. 390, *Biochemical and Biophysical Research Communications*. 2009. p. 1093–7. <https://doi.org/10.1016/j.bbrc.2009.10.093> PMID: 19853579
29. Alexander AG, Marfil V, Li C. Use of *Caenorhabditis elegans* as a model to study Alzheimer's disease and other neurodegenerative diseases. *Front Genet*. 2014 Sep 5; 5(JUL):1–21.
30. Levitan D, Doyle TG, Brousseau D, Lee MK, Thinakaran G, Slunt HH, et al. Assessment of normal and mutant human presenilin function in *Caenorhabditis elegans*. *Proc Natl Acad Sci*. 1996 Dec 10; 93(25):14940–4. <https://doi.org/10.1073/pnas.93.25.14940> PMID: 8962160
31. Hobert O. The neuronal genome of *Caenorhabditis elegans*. *WormBook Online Rev C Elegans Biol*. 2013 Aug 13; 1–106. <https://doi.org/10.1895/wormbook.1.161.1> PMID: 24081909
32. Alvarez J, Alvarez-Illera P, Santo-Domingo J, Fonteriz RI, Montero M. Modeling Alzheimer's Disease in *Caenorhabditis elegans*. *Biomedicines*. 2022 Feb; 10(2):288. <https://doi.org/10.3390/biomedicines10020288> PMID: 35203497

33. Apostolakou AE, Sula XK, Nastou KC, Nasi GI, Iconomidou VA. Exploring the conservation of Alzheimer-related pathways between *H. sapiens* and *C. elegans*: a network alignment approach. *Sci Rep*. 2021 Feb 25; 11(1):4572. <https://doi.org/10.1038/s41598-021-83892-9> PMID: 33633188
34. Milano M, Cinaglia P, Guzzi PH, Cannataro M. Aligning Cross-Species Interactomes for Studying Complex and Chronic Diseases. *Life*. 2023 Jul; 13(7):1520. <https://doi.org/10.3390/life13071520> PMID: 37511895
35. Hornsten A, Lieberthal J, Fadia S, Malins R, Ha L, Xu X, et al. APL-1, a *Caenorhabditis elegans* protein related to the human β -amyloid precursor protein, is essential for viability. *Proc Natl Acad Sci*. 2007 Feb 6; 104(6):1971–6.
36. Poorkaj P, Sharma V, Anderson L, Nemens E, Alonso ME, Orr H, et al. Missense mutations in the chromosome 14 familial Alzheimer's disease presenilin 1 gene. *Hum Mutat*. 1998; 11(3):216–21. [https://doi.org/10.1002/\(SICI\)1098-1004\(1998\)11:3<216::AID-HUMU6>3.0.CO;2-F](https://doi.org/10.1002/(SICI)1098-1004(1998)11:3<216::AID-HUMU6>3.0.CO;2-F) PMID: 9521423
37. Sherrington R, Rogaev EI, Liang Y, Rogaeva EA, Levesque G, Ikeda M, et al. Cloning of a gene bearing missense mutations in early-onset familial Alzheimer's disease. *Nature*. 1995 Jun; 375(6534):754–60. <https://doi.org/10.1038/375754a0> PMID: 7596406
38. Zhang S, Cai F, Wu Y, Bozorgmehr T, Wang Z, Zhang S, et al. A presenilin-1 mutation causes Alzheimer disease without affecting Notch signaling. *Mol Psychiatry*. 2018; 3293:1–11. <https://doi.org/10.1038/s41380-018-0101-x> PMID: 29915376
39. Evans T. Transformation and microinjection. *WormBook*. 2006;
40. Yochem J, Herman RK. Genetic mosaics. *WormBook: the online review of C. elegans biology*. s.n.]; 2005. p. 1–6.
41. Levitan D, Greenwald I. Facilitation of lin-12-mediated signalling by sel-12, a *Caenorhabditis Elegans* S182 Alzheimer's Disease Gene. *Nature*. 1995; 377(6547):351–4. <https://doi.org/10.1038/377351a0> PMID: 7566091
42. Margie O, Palmer C, Chin-Sang I. *C. elegans* chemotaxis assay. *J Vis Exp*. 2013 Apr;(74):e50069–e50069. <https://doi.org/10.3791/50069> PMID: 23644543
43. Gandhi S, Santelli J, Mitchell DH, Wesley Stiles J, Rao Sanadi D. A simple method for maintaining large, aging populations of *Caenorhabditis elegans*. *Mech Ageing Dev*. 1980 Feb; 12(2):137–50. [https://doi.org/10.1016/0047-6374\(80\)90090-1](https://doi.org/10.1016/0047-6374(80)90090-1) PMID: 6445025
44. Swierczek NA, Giles AC, Rankin CH, Kerr RA. High-throughput behavioral analysis in *C. elegans*. *Nat Methods*. 2011; 8(7):592–602. <https://doi.org/10.1038/nmeth.1625> PMID: 21642964
45. Singh K, Chao MY, Somers GA, Komatsu H, Corkins ME, Larkins-Ford J, et al. *C. elegans* Notch Signaling Regulates Adult Chemosensory Response and Larval Molting Quiescence. *Curr Biol*. 2011 May; 21(10):825–34. <https://doi.org/10.1016/j.cub.2011.04.010> PMID: 21549604
46. Link CD, Cypser JR, Johnson CJ, Johnson TE. Direct observation of stress response in *Caenorhabditis elegans* using a reporter transgene. *Cell Stress Chaperones*. 1999; 4(4):235. [https://doi.org/10.1379/1466-1268\(1999\)004<0235:doosri>2.3.co;2](https://doi.org/10.1379/1466-1268(1999)004<0235:doosri>2.3.co;2) PMID: 10590837
47. Chao MY, Larkins-Ford J, Tucey TM, Hart AC. lin-12 Notch functions in the adult nervous system of *C. elegans*. *BMC Neurosci*. 2005 Dec 12; 6(1):45. <https://doi.org/10.1186/1471-2202-6-45> PMID: 16011804
48. L'Hernault SW, Arduengo PM. Mutation of a putative sperm membrane protein in *Caenorhabditis elegans* prevents sperm differentiation but not its associated meiotic divisions. *J Cell Biol*. 1992 Oct 1; 119(1):55–68. <https://doi.org/10.1083/jcb.119.1.55> PMID: 1527173
49. Li X, Greenwald I. HOP-1, a *Caenorhabditis elegans* presenilin, appears to be functionally redundant with SEL-12 presenilin and to facilitate LIN-12 and GLP-1 signaling. *Proc Natl Acad Sci*. 1997 Oct 28; 94(22):12204–9. <https://doi.org/10.1073/pnas.94.22.12204> PMID: 9342387
50. Westlund B, Parry D, Clover R, Basson M, Johnson CD. Reverse genetic analysis of *Caenorhabditis elegans* presenilins reveals redundant but unequal roles for sel-12 and hop-1 in Notch-pathway signaling. *Proc Natl Acad Sci*. 1999 Mar 2; 96(5):2497–502. <https://doi.org/10.1073/pnas.96.5.2497> PMID: 10051671
51. Wittenburg N, Elmer S, Lakowski B, Rohrig S, Rudolph C, Baumeister R. Presenilin is required for proper morphology and function of neurons in *C. elegans*. *Nature*. 2000; 406(July):306–9. <https://doi.org/10.1038/35018575> PMID: 10917532
52. Taylor SR, Santpere G, Weinreb A, Barrett A, Reilly MB, Xu C, et al. Molecular topography of an entire nervous system. *Cell*. 2021 Aug; 184(16):4329–4347.e23. <https://doi.org/10.1016/j.cell.2021.06.023> PMID: 34237253
53. Kushibiki Y, Suzuki T, Jin Y, Taru H. RIMB-1/RIM-Binding Protein and UNC-10/RIM Redundantly Regulate Presynaptic Localization of the Voltage-Gated Calcium Channel in *Caenorhabditis elegans*. *J*

- Neurosci. 2019 Oct 30; 39(44):8617–31. <https://doi.org/10.1523/JNEUROSCI.0506-19.2019> PMID: 31530643
54. Sarasija S, Norman KR. A γ -Secretase Independent Role for Presenilin in Calcium Homeostasis Impacts Mitochondrial Function and Morphology in *Caenorhabditis elegans*. *Genetics*. 2015 Dec 1; 201(4):1453–66.
 55. Bargmann CI. Chemosensation in *C. elegans*. *WormBook: the online review of C. elegans biology*. 2006. p. 1–29. <https://doi.org/10.1895/wormbook.1.123.1> PMID: 18050433
 56. Troemel ER, Chou JH, Dwyer ND, Colbert HA, Bargmann CI. Divergent seven transmembrane receptors are candidate chemosensory receptors in *C. elegans*. *Cell*. 1995; 83(2):207–18. [https://doi.org/10.1016/0092-8674\(95\)90162-0](https://doi.org/10.1016/0092-8674(95)90162-0) PMID: 7585938
 57. Singh K, Chao MY, Somers GA, Komatsu H, Corkins ME, Larkins-Ford J, et al. *C. elegans* Notch Signaling Regulates Adult Chemosensory Response and Larval Molting Quiescence. *Curr Biol*. 2011 May; 21(10):825–34. <https://doi.org/10.1016/j.cub.2011.04.010> PMID: 21549604
 58. Sarasija S, Laboy JT, Ashkavand Z, Bonner J, Tang Y, Norman KR. Presenilin mutations deregulate mitochondrial Ca²⁺ homeostasis and metabolic activity causing neurodegeneration in *Caenorhabditis elegans*. *eLife*. 2018 Jul 10; 7:1–30.
 59. Tong YG, Bürglin TR. Conditions for dye-filling of sensory neurons in *Caenorhabditis elegans*. *J Neurosci Methods*. 2010 Apr; 188(1):58–61. <https://doi.org/10.1016/j.jneumeth.2010.02.003> PMID: 20149821
 60. Frøkjær-Jensen C, Wayne Davis M, Hopkins CE, Newman BJ, Thummel JM, Olesen SP, et al. Single-copy insertion of transgenes in *Caenorhabditis elegans*. *Nat Genet*. 2008 Nov 26; 40(11):1375–83. <https://doi.org/10.1038/ng.248> PMID: 18953339
 61. Dickinson DJ, Goldstein B. CRISPR-based methods for *caenorhabditis elegans* genome engineering. *Genetics*. 2016; 202(3):885–901. <https://doi.org/10.1534/genetics.115.182162> PMID: 26953268
 62. Shen J, Bronson RT, Chen DF, Xia W, Selkoe DJ, Tonegawa S. Skeletal and CNS Defects in Presenilin-1-Deficient Mice. *Cell*. 1997 May; 89(4):629–39. [https://doi.org/10.1016/s0092-8674\(00\)80244-5](https://doi.org/10.1016/s0092-8674(00)80244-5) PMID: 9160754
 63. Yu H, Saura CA, Choi SY, Sun LD, Yang X, Handler M, et al. APP processing and synaptic plasticity in presenilin-1 conditional knockout mice. *Neuron*. 2001; 31(5):713–26. [https://doi.org/10.1016/s0896-6273\(01\)00417-2](https://doi.org/10.1016/s0896-6273(01)00417-2) PMID: 11567612
 64. Ryan KC, Ashkavand Z, Sarasija S, Laboy JT, Samarakoon R, Norman KR. Increased mitochondrial calcium uptake and concomitant mitochondrial activity by presenilin loss promotes mTORC1 signaling to drive neurodegeneration. *Aging Cell*. 2021 Oct 9; 20(10):1–18. <https://doi.org/10.1111/accel.13472> PMID: 34499406
 65. Brai E, Alina Raio N, Alberi L. Notch1 hallmarks fibrillary depositions in sporadic Alzheimer's disease. *Acta Neuropathol Commun*. 2016 Jul 1; 4(1):64. <https://doi.org/10.1186/s40478-016-0327-2> PMID: 27364742
 66. Greenwald IS, Sternberg PW, Horvitz HR. The *lin-12* locus specifies cell fates in *caenorhabditis elegans*. *Cell*. 1983 Sep 1; 34(2):435–44. [https://doi.org/10.1016/0092-8674\(83\)90377-x](https://doi.org/10.1016/0092-8674(83)90377-x) PMID: 6616618
 67. Eimer S, Donhauser R, Baumeister R. The *Caenorhabditis elegans* presenilin *sel-12* is required for mesodermal patterning and muscle function. *Dev Biol*. 2002 Nov 1; 251(1):178–92. <https://doi.org/10.1006/dbio.2002.0782> PMID: 12413907
 68. Ferguson EL, Horvitz HR. Identification and characterization of 22 genes that affect the vulval cell lineages of the nematode *Caenorhabditis elegans*. *Genetics*. 1985 May; 110(1):17–72. <https://doi.org/10.1093/genetics/110.1.17> PMID: 3996896